SECOND LAW ANALYSIS OF DOUBLE PASS SOLAR AIR HEATER EQUIPPED WITH ALUMINUM RECYCLED CANS AS AUGMENTATION TECHNIQUES

2022
MASTER THESIS
MECHANICAL ENGINEERING

HAITHAM GHASSAN YASEEN

Thesis Advisors

Prof. Dr. Mehmet ÖZALP

Assist.Prof.Dr. Wissam H. KHALIL

SECOND LAW ANALYSIS OF DOUBLE PASS SOLAR AIR HEATER EQUIPPED WITH ALUMINUM RECYCLED CANS AS AUGMENTATION TECHNIQUES

Haitham Ghassan YASEEN

T.C.
Karabuk University
Institute of Graduate Programs
Department of Mechanical Engineering

Prepared as
Master Thesis

Thesis Advisors
Prof. Dr. Mehmet ÖZALP
Assist. Prof. Dr.Wissam H. KHALIL

KARABUK
August 2022

I certify that in my opinion the thesis submitted by Haitham Ghassan YASEEN titled "SECOND LAW ANALYSIS OF DOUBLE PASS SOLAR AIR HEATER EQUIPPED WITH ALUMINUM RECYCLED CANS AS AUGMENTATION TECHNIQUES" is fully adequate in scope and quality as a thesis for the degree of Master of Science.

Prof. Dr. Mehmet ÖZALP .....
Thesis Advisor, Department of Mechanical Engineering
Assist. Prof. Dr. Wissam H. Khalil .....
Thesis Co-Advisor, University of Anbar

This thesis is accepted by the examining committee with a unanimous vote in the Department of Mechanical Engineering as a Master of Science thesis. 24.08.2022

Examining Committee Members (Institutions)	Signature
Chairman : Pof. Dr. Mehmet ÖZALP	.....
Member : Dr. Öğr. Üyesi Cevat ÖZARPA	.....
Member : Doç. Dr. Volkan KIRMACI	.....

The degree of Master of Science by the thesis submitted is approved by the Administrative Board of the Institute of Graduate Programs, Karabuk University.

Prof. Dr. Hasan SOLMAZ .....
Director of the Institute of Graduate Programs

"I declare that all the information within this thesis has been gathered and presented in accordance with academic regulations and ethical principles and I have according to the requirements of these regulations and principles cited all those which do not originate in this work as well."

Haitham Ghassan YASEEN

ABSTRACT

M. Sc. Thesis

SECOND LAW ANALYSIS OF DOUBLE PASS SOLAR AIR HEATER EQUIPPED WITH ALUMINUM RECYCLED CANS AS AUGMENTATION TECHNIQUES

Haitham Ghassan YASEEN

Karabük University
Institute of Graduate Programs
The Department of Mechanical Engineering

Thesis Advisor:
Prof. Dr. Mehmet ÖZALP
Assist. Prof. Dr. Wissam H. Khalil
August 2022, 76 pages

The global fuel crisis and its environmental damage prompted many researchers to develop solar air heaters used in heating applications and drying agricultural crops. The current study included the development of the performance of the solar air heater using the extended surfaces represented by hollow cans. An experimental setup of double pass solar air heater collector was fabricated and equipped with the necessary equipment's needed foe measurement. Three models were used in this study. In model I; No modifications have been made to the flat plate that absorbs sunlight. In model II; The hollow recycled aluminum cans, which have two different diameters and lengths, are arranged in equally spaced rows, one after the other, in such a way that air enters and parallel to the direction of the flow, regardless of the fact that they have the same dimensions. In model III, the same sorting process was performed in model II, but taking into account the fact that the cans to be lined up are the same.The experiments were conducted in Anbar Governorate - Ramadi climatic conditions. Four values of the mass air flow rate were used to show its effect on the performance of these

collectors. The effect of changing the values of solar radiation on the performance of these collectors was studied. the results showed that as the solar irradiation increases the thermal efficiency increases and the thermal efficiency is greatly dependent to the mass flowrate. at midday the highest value of temperature difference (7°C) , the highest thermal efficiency (75.9 %) and The second law thermal analysis gave the highest exergetic efficiency (38.57 %) was obtained by using Model II. The comparison with previous published data gave a good agreement.

Key Words : Double Pass, Solar Air Heater, Thermal Efficiency, Mass Flow Rate, Solar Radiation.

Science Code : 91408

ÖZET

Yüksek Lisans Tezi

GERİ DÖNÜŞÜMLÜ ALÜMİNYUM KUTULAR İLE DONATILMIŞ ÇİFT GEÇİŞLİ GÜNEŞ ENERJİLİ HAVA ISITICISININ BÜYÜTME TEKNİKLERİ OLARAK İKİNCİ KANUN ANALİZİ

Haitham Ghassan YASEEN

Karabük Üniversitesi
Lisansüstü Eğitim Enstitüsü
Makina Mühendisliği Anabilim Dalı

Tez Danışmanı:
Prof. Dr. Mehmet ÖZALP
Assist. Prof. Dr. Wissam H. Khalil
Ağustos 2021, 77 sayfa

Küresel enerji krizi ve enerji üretmek için kullanılan yakıtın çevreye verdiği zararlardan dolayı, birçok araştırmacıyı ısıtma uygulamalarında ve tarımsal ürünlerin kurutulmasında kullanılan güneş enerjili hava ısıtıcıları geliştirmeye yönlendirmiştir. Bu çalışmada, güneş ışığı emen düz plakanın güneş ışığına ve üflenen havaya maruz kalan alanını içi boş geri dönüşümlü alüminyum kutularla değiştirerek oluşturulan güneş enerjili hava ısıtıcısının bu değişimlerden dolayı performansında oluşan gelişmeler incelenmiştir. Çift geçişli güneş enerjili hava ısıtıcı kollektör deney düzeneği literatürde bulunan ekipmanların dış ölçülerine göre imal edilmiştir. Bu çalışmada üç model kullanılmıştır. Model I'da; güneş ışığını emen düz plakaya herhangi bir değişiklik yapılmamıştır. Model II'da ise; iki farklı çaplara ve uzunluklara sahip olan içi boş geri dönüşümlü alüminyum kutular aynı ebatlara sahip olmasının

dikkate almayarak içinden hava girecek ve akışın yönüne paralel olacak şekilde arka arkaya eşit aralıklı sıralar halinde dizilmiştir. Model III'da ise model II'de yapılan dizme işleminin aynısı fakat dizilecek olan kutuların aynı olması dikkate alarak yapılmıştır. Denemeler Anbar Valiliği - Ramadi iklim koşullarında gerçekleştirilmiştir. Bu kollektörlerin performans değişimi göstermek için dört farklı kütlesel debi kullanılmıştır. Güneş ışığı değerlerinin değiştirilmesiyle birlikte kollektörlerin performansına oluşan etki incelenmiştir. Sonuçlar, güneş ışığı şiddeti arttıkça termal verimliliğin arttığını ve termal verimliliğin büyük ölçüde kütle akış hızına bağlı olduğunu göstermiştir. Öğle saatlerinde en yüksek sıcaklık farkı değeri (7°C), en yüksek ısıl verim (%75.9) ve ikinci kanun ısıl analizi en yüksek ekserjetik verimi (%38.57) Model II kullanılarak elde edilmiştir. Bu elde edilen veriler daha önce literatürde yayınlanmış verilerle karşılaştırıldığında sonuçların mantıklı olduğunu ve deneyin doğuru yapıldığını tespit edilmiştir.

Anahtar Kelimeler : Çift Geçişli, Güneş Enerjili Hava Isıtıcı, Termal Verimlilik, Kütle Akış Hızı, Güneş Radyasyonu.

Bilim Kodu **:** 91408

ACKNOWLEDGMENT

At the beginning, I would like to express my gratitude and thanks to the Creator, the Almighty, for his grace and from him who helped me in my work, as well as my thanks and appreciation to my first supervisor, Prof. Dr. Mehmet ÖZALP for everything he gave me. Also, I would like to extend all words of thanks and gratitude to my second supervisor, Assist. Prof. Dr. Wissam H. Khalil, without whom I would not be where I am today. I also extend my thanks and appreciation to Anbar University, especially the Renewable Energy Research Center, headed by the Director of the Center, Dr. Wissam Hashem Khalil, as well as all the center's staff including professors, administrators, and officials, for the facilities they provided me with providing a helping hand, and using laboratories and some equipment. They have all my love and respect.

My thanks to my family, brothers and sisters, and especially to my father's soul, how much you wished now with me, but God's destiny, may God have mercy on you and my loving mother with her blessing I walk and the virtue of her supplication for me.

My thanks to my dear wife who took responsibility with me and for what she gave me.

My thanks to my children as they always pray for me.

My thanks to all my friends, especially my dear friend Omar Mohamed Fakhry, for standing with me in accomplishing my study.

My thanks also to my friend Omar Noureddine, who was the reason for accepting me and completing all the required work.

Thanks to all the relatives and loved ones.

CONTENTS

Page

Page

Page

LIST OF FIGURES

Page

Page

LIST OF TABLES

Page

SYMBOLS AND ABBREVIATIONS

SYMBOLS

A : Cross sectional area of duct

A_b : The area of absorber plate

b : Width of collector

C_b : Specific heat

D_b : Hydraulic diameter

EX_{in} : exergy inlet

EX_{out} : Exergy outlet

F : Friction factor

H : Height of collector

H_{in} : Enthalpy inlet of air

H_{out} : Enthalpy inlet of air

I : Total solar radiation incident in the collector

K : Thermal conductivity

L : Length of collector

m : Mass flow rate

P : Perimeter of duct

P_{in} : Pressure inlet

P_{out} : Pressure outlet

Q_s : Solar energy absorbed by the collector

Q_u : Useful heat gain

Re : Reynold number

S_{out} : Entropy outlet of air

S_{in} : Entropy inlet of air

T_{out} : Temperature outlet

T_{ave} : Average temperature

T_e : Environment temperature

T_{in} : Temperature inlet

T_s : Absorber plate temperature

V : Air velocity at the collector inlet pipe

Δ : Difference

$\Delta\rho$: Pressure drops

$\Delta\rho f$: Pressure drop due to friction losses

$\Delta\rho f_{other}$: Pressure drop due to minor losses

ΔT : Temperature difference

μ : Dynamic viscosity

α : Absorptivity

ε : Emissivity

$\aleph_{Ex}$: Exegetic efficiency

ρ : Air density

τ : Transmissivity

A : Air

Ave : Average

e : Environment

In : Inlett

Out : Outlet

ABBREVIATIONS

CFD : Computational Fluid Dynamics

DPSAC : Double Pass Solar Air Collector

DPSAH : Double Pass Solar Air Inlet

FEM : Finite Element Method

FPSAH : Finned Plate Solar Air Heater

PCM : Phase Change Materials

SAH : Solar Air Heater

SPSAH : Single Pass Solar Air Heater

TCM : Thermal-Chemical Storage

TES : Thermal Energy Storage

TESD : Thermal Energy Storage Device

TSM : Thermal Storage Materials

PART 1

INTRODUCTION

1.1. OVERVIEW

Energy is a critical source of economic growth in agriculture, manufacturing, and a variety of other industries. The increased usage of conventional energy resulted in increased pollution and its negative impact on the environment. Fossil fuel use leads to pollution of the environment and the spread of diseases that may be fatal to people. Human population growth has led to an increase in energy demands, economic and technological advancement, industrialization, and energy consumption. Researchers have shifted their attention to other forms of energy as a consequence of this. As a renewable energy source, solar energy has played an important role in history since solar energy technologies are both economical and environmentally friendly. There are a variety of ways to gather energy from the sun, but the most common method is via the use of solar collectors [1].

In the twenty-first century, the newest studies show an increment of concentration noxious gases such as nitrous oxide N_2O and carbon dioxide CO_2 in the atmospheric. An unprecedented increase in the past decades that cause global warming phenomena. The fossil fuels such as oil, gas, and coal were used to generate conventional energy in all the world. This causes many dangerous lung illnesses that endanger the life of humanity, if this problem is not dealt with seriously[2]. On the other hand, fossil fuel resources are beginning to run out unprecedentedly in recent years due to the overuse. The rising expense of traditional fossil fuels prompted the researchers to look for other energy sources. To lessen the environmental effect of fossil fuel consumption, many countries are making attempts to set up systems for generating renewable energy.

The energy crisis and global warming drive to get an alternative way to overcome conventional fossil fuel problems. Renewable energy represents the principal solution, to meet the demand of energy and decreases the CO_2 and N_2O emissions that decrease the greenhouse effect [3].

Solar, wind, tidal, and water are examples of renewable sources of energy that can be renewed by nature. Solar power is becoming the most common form of energy generation. Earth receives an estimated 174 000 TW of solar energy from the sun, which is 40 000 times more than humans require [4].

The heat and light generated by sun source are converted into electrical energy and various thermal applications. The advantages of solar energy system are : available, Eco friendly, low maintenance cost, no fuel cost, etc. For both residential and commercial use, solar air heaters (SAH) are a popular option. A solar air heater, on the other hand, is a device that utilizes solar energy to generate heat energy. This device is simple to build and inexpensive to produce.

1.2. PROBLEM STATEMENT

Focusing on solar energy, as previously mentioned, and reducing harmful emissions to the outside atmosphere has generated an urgent need for such studies. The problem statement of such study represents the following issues:

1. The second rule of thermodynamics states, a significant amount of attention has been focused, over the course of the last two decades, on the thermal performance of solar collectors that use a double-pass configuration.
2. Due to limited thermal conductivity, researchers must utilize heat transfer enhancement technologies to increase heat exchange between solar collector absorber plates and air.
3. In order to reduce the cost of manufacturing solar collectors, researchers benefited from reusing metal cans as flow and heat transfer augumentated techniques inside the solar collector, and this idea helps to reuse wasted materials such as cans in useful things and reduce its accumulation.

1.3. OBJECTIVES

The following is a list of the study's primary goals:

1. To investigate experimentally the mechanism of heat transfer of solar radiation within double-pass solar air heater.
2. To conduct a comparison between the augmented absorber plates with recycled cans with respect to the traditional plates.

1.4. SCOPE

In this experimental study, three models of SAH were used. Furthermore, the first model consists of flat absorber plate only, while in the second and third model cans augmented on the absorber plate oriented in two different orientations. The experiments were carried out in Ramadi city, Iraq's Anbar Governorate is located at a height above sea level of 59.8 m, with a longitude of 43.268° east and a latitude of 33.43° north. Also, experiments were performed during winter season: February and March 2022. Experiment time was from 09:00 am to16:00 pm. The collector's direction is to the south with an angle of 45°.

1.5. THESIS OUTLINE

This thesis is divided into five sections. The first chapter provides an introduction of the topic as well as an explanation of each issue problem, purpose, and research area. The second chapter presents the required basic theoretical aspects to perform the experimental work. Besides, the available studies dealt with this subject were discussed also. The third chapter introduces the practical system, how to manufacture the considered models, how to operate, and how data were collected as well as how data were analyzed. In the fourth chapter, the collected data were presented along with comparisons made between the models in order to highlight the best tested model. Finally, Chapter five summarizes the significant conclusions, recommendations and

PART 2

LITERATURE REVIEW

2.1. INTRODUCTION

In this chapter, the Solar Air Heater Collectors (SAHs) is reviewed along with its practical applications. The types of SAHs were presented as well. Besides, the present available studies dealt with improving the thermal efficiency of the SAHs were discussed thoroughly.

2.2. SOLAR AIR HEATER COLLECTOR

A heat exchanger is used to heat the working fluid on a solar collector's absorber plate. Solar air collectors consist of an absorber plate, air passages, side and bottom insulation, and transparent covers. The solar air heater has a wide range of uses, including room heating, air conditioning, agricultural product drying, water heating, and industrial process heating, to name a few [5]. There are many advantages of solar air heating, as listed below:

1. They are simple to design and maintenance.
2. No fuel used.
3. Compared to the systems that utilize the liquid there are smaller leakage and corrosion.
4. No greenhouse gas emissions.
5. Eco-friendly system.

Due to a weak convective-coefficient between the air moving and the absorbent plate and the loss of energy to the environment, solar air collectors have poorer thermal efficiency than conventional collectors. Flat plate-absorbent surface design is the first

type of SAHs that may be categorized into two subcategories based on their ability to increase solar air collector performance. The darkened plate is used to improve airflow turbulence and convection area. Extended surfaces, such as (fins/obstacles), wire screens as porous materials, roughened or grooved surfaces, may improve the thermal efficiency of SAHs, see Figure 2.1.

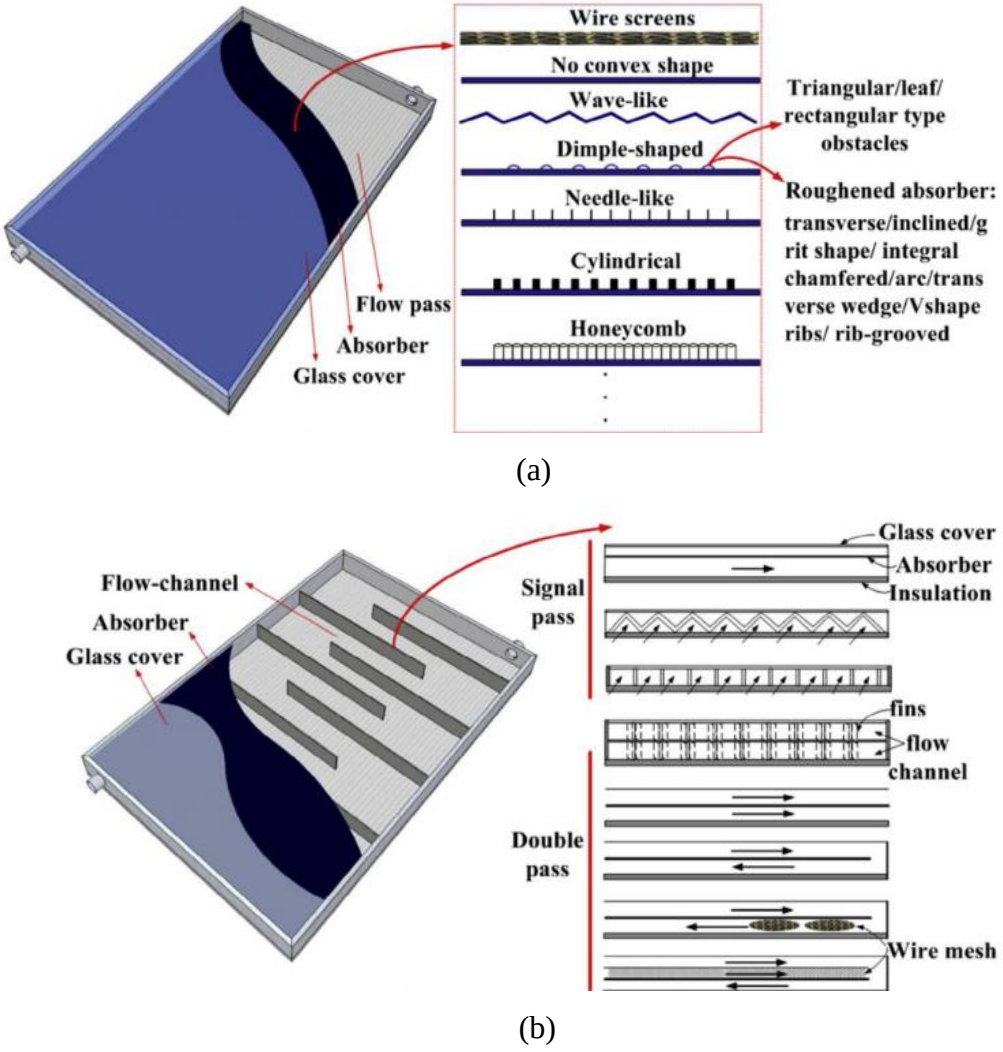

Figure 2.1. Flat plate-SAHs configurations:(a) Absorber surface design, and (b) Channel flow patterns [5].

Absorbent surface design that minimizes energy losses to the environment, including the number of air passages and the kind of air flow over the absorbent surface, as shown in Figure (2.2) are the second group of factors [5]. As a point of reference, the collector in this investigation was a single-flow, double-pass design with an extended

absorber plate. SAH's thermal efficiency and output temperature are strongly influenced by the airflow channel model. There are four primary types of SAH setups:

- Model (I) a front flow-single pass heater
- Model (II) a back flow-single pass heater
- Model (III) a parallel flow-double pass heater
- Model (IV) a counter flow-double pass heater, as shown in Figure (2.2).

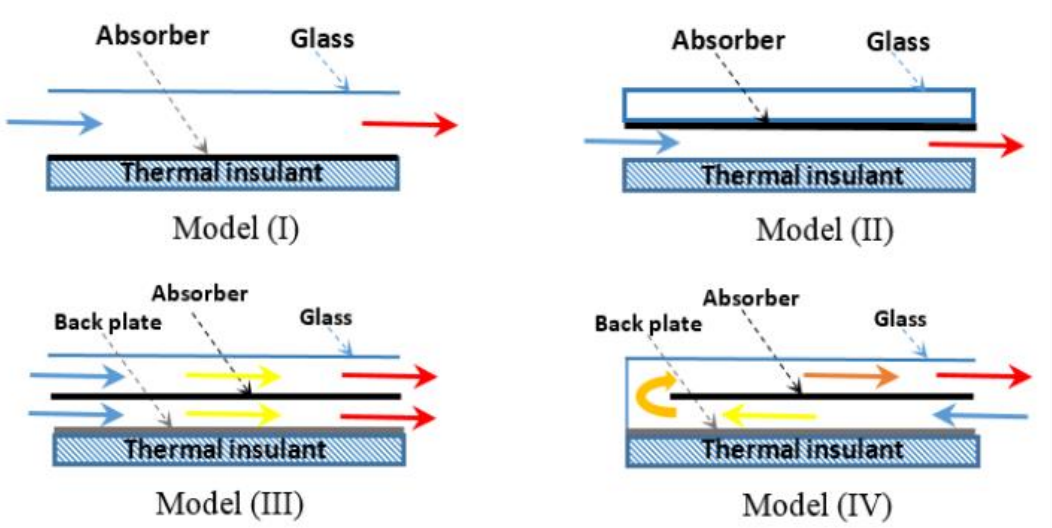

Figure 2.2. Airflow pass types of a flat plate-SAHs [5].

Thermal engineers have used solar air collectors widely in several applications. Sunlight and more energy being transmitted to air moving through a channel raises air temperature as a result of this absorber plate and channel. As a result, this warm air may be used to a variety of uses, including: heating homes, public buildings, workplaces, and agricultural products through solar drying, for example (paddy grains, fruit, etc.). Making the crop direct and dehydrating it with sun radiation may save energy by protecting it from rodents, damage, and the like. It may also be utilized in industrial heating procedures (the procedure of preparing air for burning by heating it up to a temperature above ambient, dehydrating a variety of materials, including wood, paper, and food. drying brown coal in particular, which is important for power plants).

2.3. DOUBLE PASS SINGLE FLOW SOLAR COLLECTORS

The bottom channel receives air straight from the top channel at the channel edge and flows through it. Hence the name "single flow double pass" for this kind. It is illustrated in Figure that the absorber plate is used to separate the bottom and upper channels (2.3).

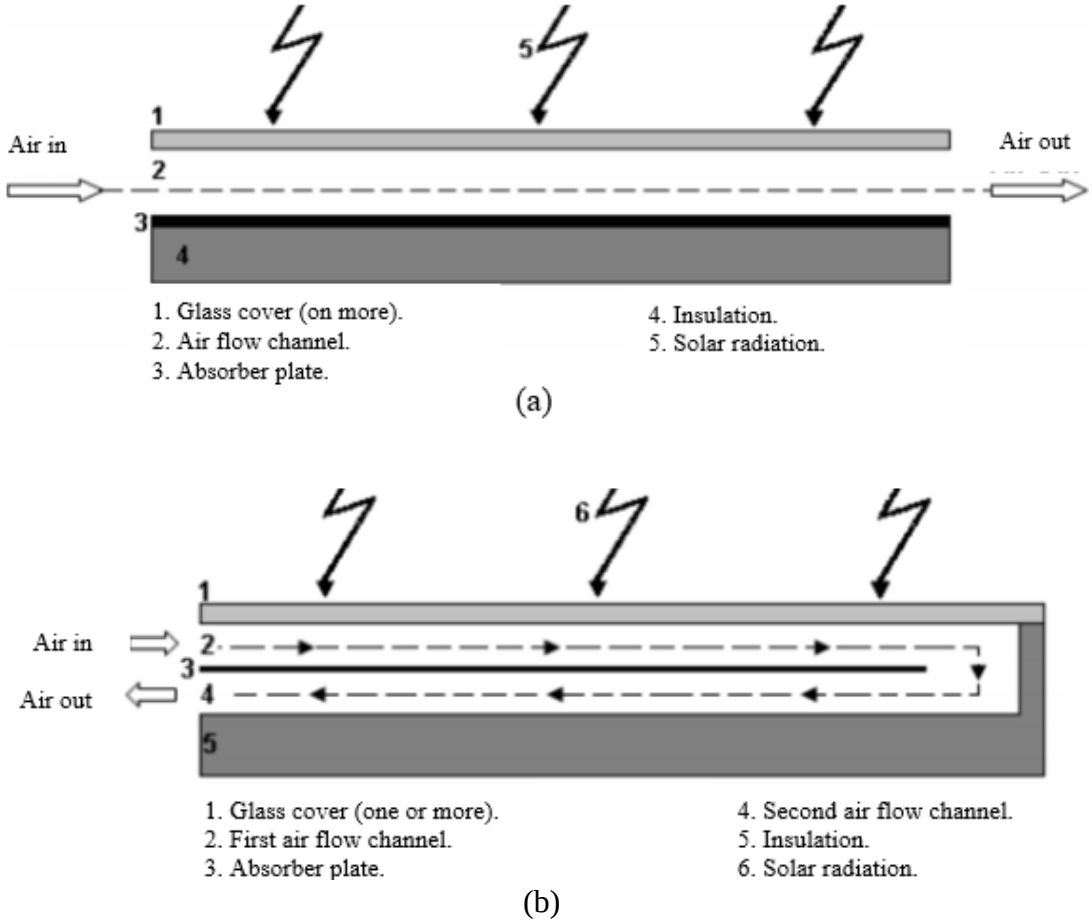

Figure 2.3. Schematic of solar collector: (a) single pass, and (b) double pass.

The absorber plate and glass cover make up the top channel, while the lower absorber plate and the insulated lower base make up the bottom channel. Solar collectors with double-pass flow and solar collectors with single-pass flow are compared in this study. It would find that the double pass flow is characterized by the presence of two flow channels, while the single-pass flow one channel and thus the double pass is more efficient than the conventional collector with a single pass, and the temperature of the output air from the flow with two passes is greater than when using only one pass than

the temperature of the single-pass flow. The reason for the increase in temperature of the air outside in the double-pass solar collector is that the air takes a longer period to exit from the collector than the single-pass collector.

2.4. ENHANCEMENT OF THERMAL ENERGY

In the open literature there are many studies dealt with the problem of enhancing thermal efficiency of SAHs. However, these studies could be divided into two categories, the first is the single pass single flow, and the second is double pass single flow. The following sub-sections describe each category individually.

2.4.1. Single Pass Single Flow

In this study [6], turbulators and exterior mirrors were examined experimentally for their impact on a newly developed single pass Solar Air Heater (SAH). The heater's efficiency was improved by stacking aluminum cans on top of the absorber plate and using them as turbulators. Studies are being conducted to determine how external bottom and top mirrors affect SAH performance. A total of three different absorbent plate designs have been put to the test when they were first conceptualized. All three are flat plates with cans (turbulators) arranged in an aligned or staggered manner. The modified SAH air heaters with and without reflectors were put to the test against a normal SAH to see which one was more efficient. Air Mass Flow Rate (MFR) varies from 0.02 to 0.05 kg/s in most cases. The suggested SAHs had a maximum daily efficiency of 73.4% at 0.05 kg/s, according to the findings. Two different types of absorbent plates were put to the test in this study. Figures 2.4 and 2.5 exhibit images of solar air heaters that have been tested, while Figure 2.5 provides a schematic for a solar air heater that has been updated. for exterior reflectors and guiding vanes on a staggered heater.

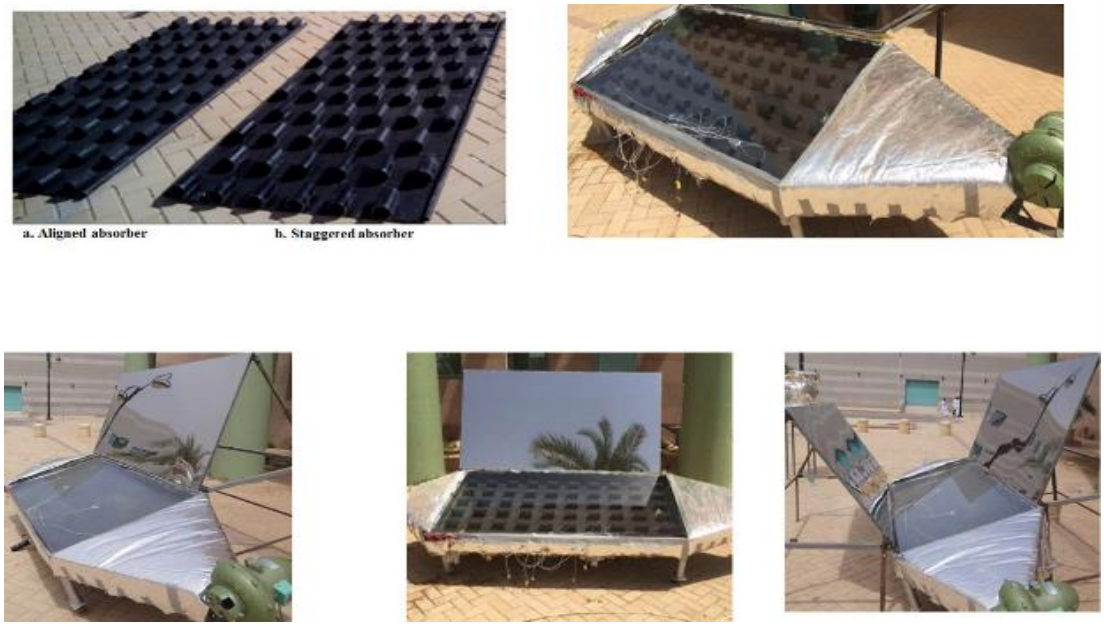

Figure 2.4. Photos of tested air solar heater [6].

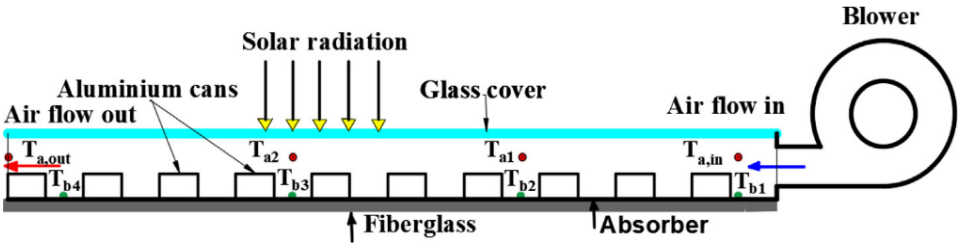

Figure 2.5. A diagram of a solar air heater that has been tested [6].

In this study [7], In an experiment, a single-pass Solar Air Heater (SAH) with nineteen longitudinal fins has been adjusted at the entry to increase performance. The air flow was distributed evenly across the channel thanks to the longitudinal fins, which increased the surface area available for heat transmission. Fin height (3, 5, and 8 cm) was studied experimentally at three different fin heights (3, 5, and 8 cm). A total of four different (m) speeds were used in the studies, which ranged from 0.013 kg/s to 0.004 kg/s. There is a daily efficiency improvement of 10% to 14% over the regular finned SAH and 18.53–24.95% finned glazed-bladed SAH with a fins height of 8 cm is an improvement over the typical heater.

Figure 2.6. Photo of the test-rig [7].

This study [8], provides a proposal for a solar air heater that only requires one pass through the system and boosts thermal efficiency by replacing the absorber plate with a matrix of wire meshes and fins. it's the city of Famagusta; Steel wire mesh with a cross sectional hole of 0.18 x 0.18 cm and a diameter of 0.02 cm replaced the absorber plate. Black paint was used to paint the fins, which were then positioned transversely down the bed to form four portions with equal spacing. As air mass flow rate rises from 0.011 kilograms per second to 0.032 kilograms per second, the thermal efficiency improves. The temperature disparity as the air mass flow rate increased, the distance between the exit air flow and the surrounding environment reduced. Figure 2.7 depicts a schematic representation of an experiment's set-up.

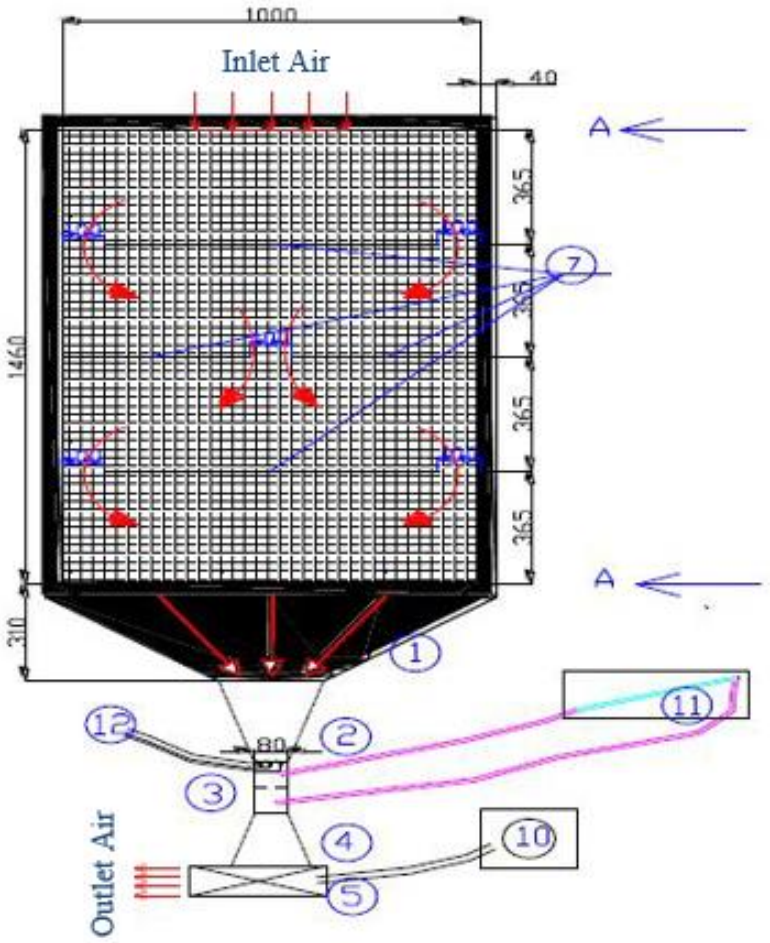

Figure 2.7. Schematic assembly of the SAH system [8].

This study [9], A single-pass semi-flexible foil duct may be introduced directly as an absorber in a solar air heater to improve its thermal performance (SAH). To assess the novel material's heating capability, tests were run at 0.013 kg/s, 0.03 kg/s, and natural convection. Experiments were compared to flat plate absorbers. One-pass semi-flexible foil duct with curved inner surface and vast surface area was more effective than flat plate duct. This was the case because of the unique combination of these two features. Figure 2.8 depicts the heaters in cross-section, as well as the test setup for forced and natural convection. Figure 2.8 shows the thermal picture of the experimental settings. In Figure 2.8, you can see the sensor locations for the arrangement.

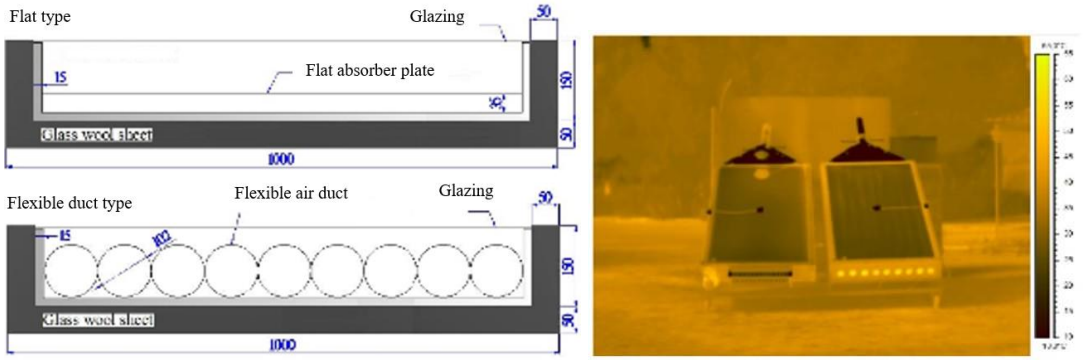

Figure 2.8. Natural and forced convections are studied in this experiment [9].

2.4.2. Double Pass Single Flow

[10] Aluminum cans were put on the absorber plate to increase fluid velocity and promote heat transmission between the plate and airflow. This study created two absorber plates. First type employs an absorber plate without cans; second type includes zigzag-shaped cans. Figures 2.9 a and b depict the A- and B-models, respectively. Single-duct double-pass collectors are used here. To reach the output duct, air must first flow through an inlet and an absorber plate before returning to the inlet. A 4 mm thick layer of glass covers the plate. Circulation of air is accomplished by the use of an axial fan. Aluminum cans arranged in a zigzag pattern raise temperatures by 3 to 10.5 degrees Celsius, according to this research. Between Types I and II, there is a 20% gain in thermal efficiency. In addition, the difference in thermal efficiency between the two models is around 3% at an average mass flow rate of 0.075 kg/s.

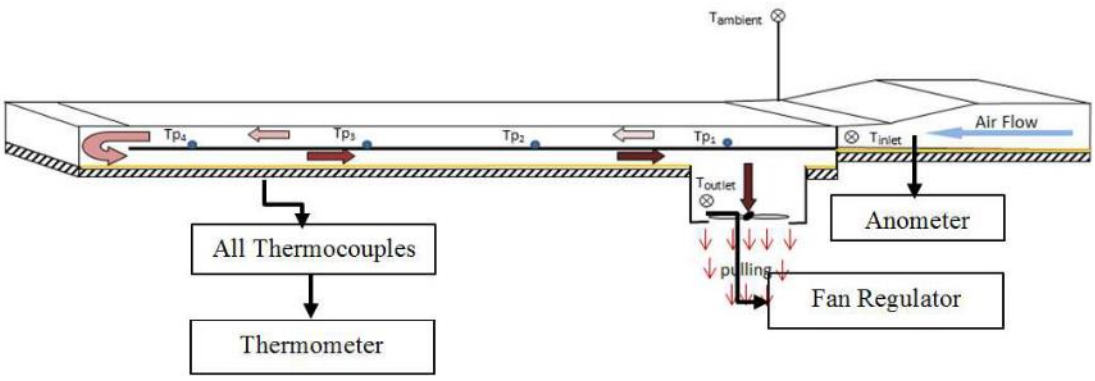

(a)

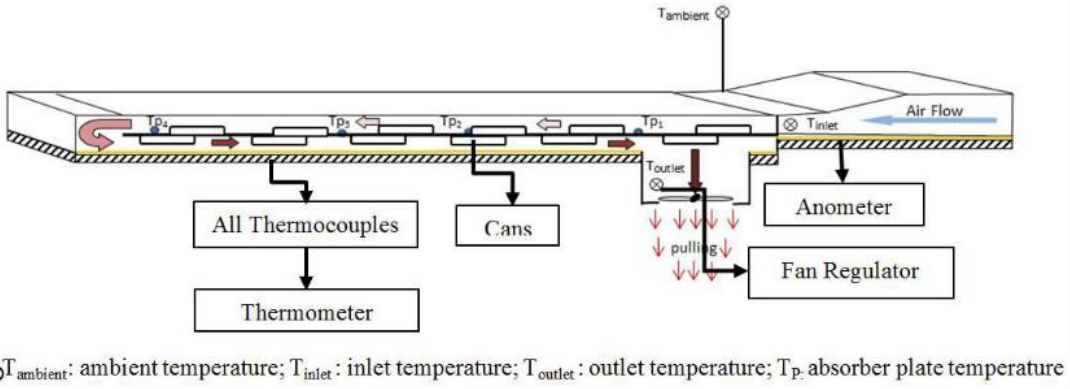

(b)

Figure 2.9. Examined models (a) model I flat absorber plate, (b) absorber plate with cans [10].

[11,12]Putting aluminum cans on top of the absorber plate of a double-pass solar collector during an experiment will enhance fluid velocity, Improved airflow and heat transfer coefficients will result as a result of this. In this research, three different kinds of absorber plates were developed. The first kind of absorber plate has cans arranged in a zigzag pattern. As shown in Figure 2.10, the absorber plates of the two other varieties were placed in a straight line, whereas the third form only employed a flat plate. Mass flow rates of 0.03 kg/s and 0.05 kg/s were used in the studies. According to the findings, using aluminum cans improved thermal efficiency by expanding the area on which heat may be transferred. The prototype model's solar air heater efficiency peaked at a mass flow rate of 0.05 kg/s. Model I (staggered cans) often outperforms Model III (flat-plate collectors) in efficiency tests (without cans). The solar collector's dead zones are minimized because of the barriers or cans, which prevent air from flowing freely over and under the absorber surfaces.

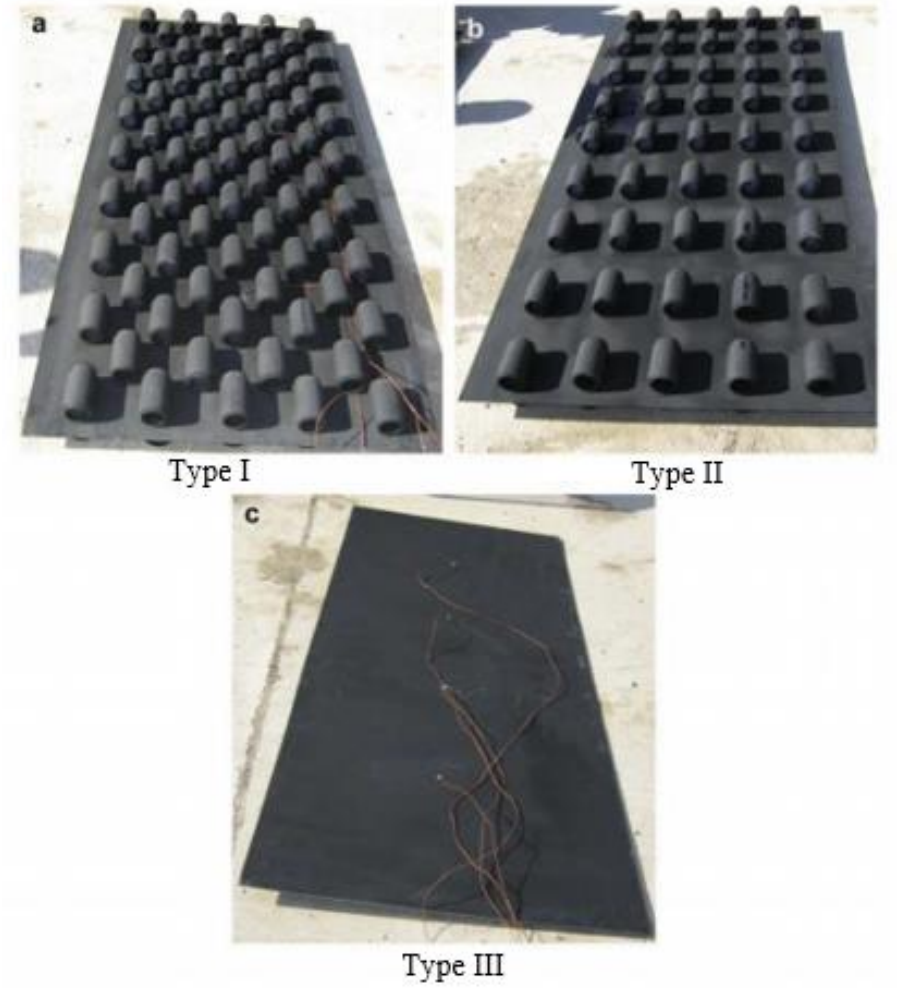

Figure 2.10. The configurations of the absorber plate 2 [11,12] .

In [13], experimented with the surface extension approach to see if it may help. Solar air heaters with thermal energy storage systems are being developed and tested in Iraq-Baghdad climatic conditions to store additional solar electricity and release it at night. Several frigid winter days in January, February, and March of 2016 were used to test the charging and discharging characteristics of the new system at air mass flow rates ranging from 0.025 kg/s to 0.06 kg/s. 4.5 hours after sunset, the average exit air temperature was 8.2 °C warmer than the input temperature due to thermal storage medium present at the absorber plate, according to the results of the research. With a low mass flow rate, the storage system's capacity may be used to its full potential and heat can be supplied for a longer period of time. Also, the air mass flow rate of 0.03 - 0.04 kg/s is a good range for maximizing efficiency and gaining usable heat. For a mass flow rate of 0.04 kg/s, the SAHWS and SAHOS achieved maximum average efficiencies of 90 percent and 61 percent, respectively. The greatest temperature

difference between the intake and exhaust occurs at a mass flow rate of 0.025 kg/s and output air flow of paraffin wax is 41.4°C.

After carrying out research on an experimental SAH with and without obstructions, A brand-new kind of solar air heater with a flat plate has been created [14]. This contrasted with as a result, we measured the intake and Exit, absorbing plate, ambient, and solar radiation temperatures. Figure 2.11 shows the results of testing various air flow rates, ranging from 0.015 kg/s to 0.25 kg/s, using varying densities of absorbent plates in the channel duct. (10, 20, and 30 cm below the glass cover).

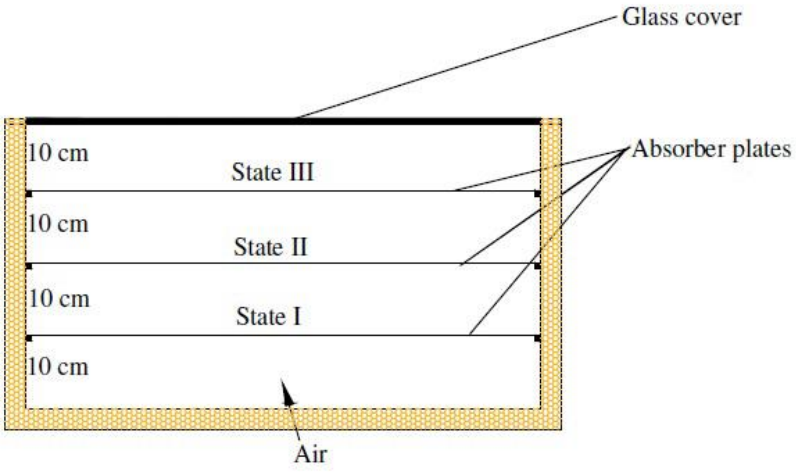

Figure 2.11. Absorber plate positions [14].

Figure 2.11 shows the four kinds of absorber plates that were used in this investigation. Comparing findings from obstructions and those from a collector provided the double-flow solar air collector that does not have obstructions has also been conducted. Figure 2.12 shows the various absorbent plates in use. Black stainless-steel dampers are used. Chrome plating that is only applied to certain areas. Dimensions and thickness of the board 1.25 m, 0.8 m, and 1 mm for each of the four collectors. The thickness of normal window glass was 5 mm. Cover glass for all four collectors was utilized; Cross-delivery Insulator (thickness 3 cm) and wind losses are the primary causes of heat loss via the appearance Collector. Insulation Slim absorbs heat radiation.

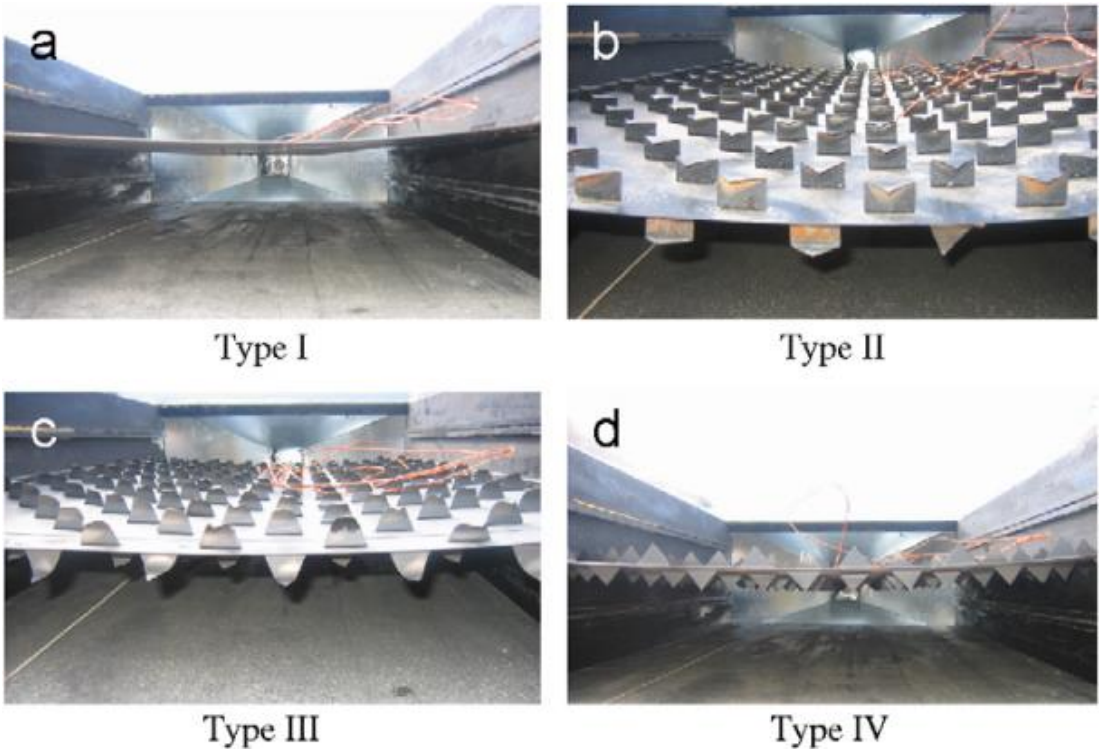

Figure 2.12. Types of absorber plates [14].

Also [15], evaluated the results of an experiment to see whether adding aluminum cans to a double-pass solar collector would improve its efficiency. SAH absorber plates may be inexpensively constructed by inserting a flat-plate double-pass channel and an aluminum can as an absorbing plate. Type I cans were staggered as if on an absorber plate, but Type II cans were stacked in a zigzag pattern. Type I cans. This kind of baffled flat plate is called Type III. At the same flow rate, the double pass's efficiency beats the single pass's by a wide margin. Aluminum sheet with a black selective coating was used to make the absorbers. Dimensions and plate thickness were 1 mm, 1 mm, and 2 mm for each of the three collectors. 4 mm thick glass was used for the glazing of this project. All three collectors utilized the same kind of cover glass.

Double-pass air heaters are tested. Double-pass solar air heaters decrease top cover heat loss across a wide mass flow range. Aluminum cans boost the effectiveness of a double-pass solar air heater. Double flow solar air heaters offer a greater output temperature for the same mass flow rate.

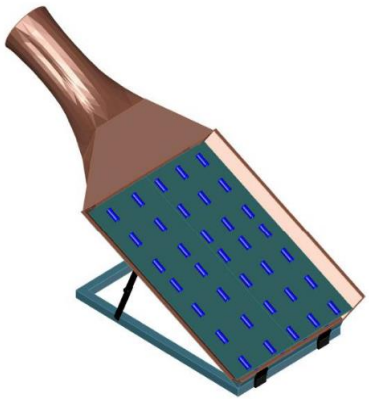

Figure 2.13. Solar air heater [15].

Figure 2.14. Photograph of Type I arrangement in double solar air heater with aluminum cans [15]

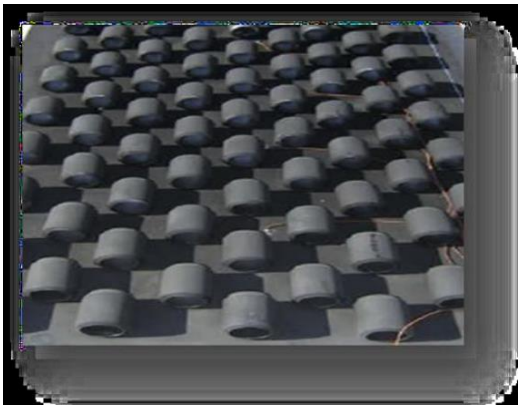

Figure 2.15. Photograph of Type II arrangement in double solar air heater with aluminum cans [15].

Figure 2.16. Photograph of Type III arrangement in double solar air heater with aluminum cans [15] .

Besides, [16], Experimental research was conducted to investigate five fins attached to the absorber plate of a single-pass solar air heater's thermal performance. The effectiveness of solar air heaters as a source of heat will be the subject of a forthcoming investigation. An experiment using solar collectors that either had or did not have fins linked to the absorber plate was conducted and is shown in Figure 2.18. Solar air collector efficiency is largely determined by a number of factors, including mass flow rate, the shape of the collector surface, the amount of solar radiation, and the presence or absence of absorber plate fins. Because of the higher air flow heat transfer at mass flow rates between 0.012 and 0.016 kg/s, the collector's efficiency improves as the amount of solar radiation that strikes it does too. The solar air collector's efficiency has been demonstrated to be greater. Collector efficiency and air temperature increase were best with a 45-degree tilt angle for the finned collector and lowest with one that didn't have fins. Double-pass air heater efficiency is tested. Over a wide range of mass flow rates, a double pass solar air heater reduces top cover heat loss. Aluminum cans boost the effectiveness of a double-pass solar air heater. Double flow solar air heaters offer a greater output temperature for the same mass flow rate.

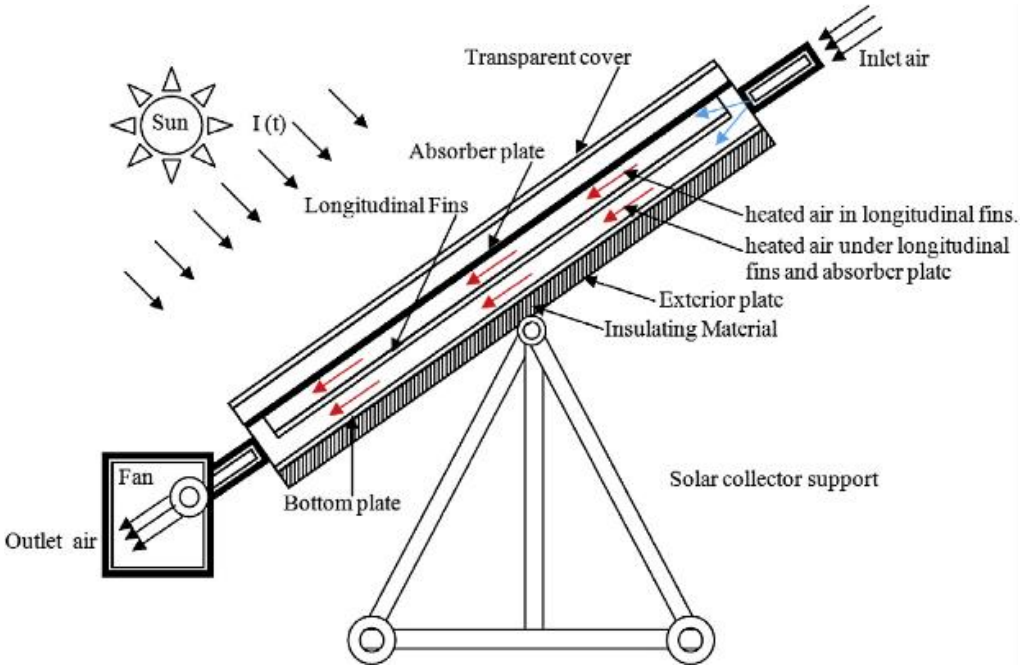

Figure 2.17. The solar air collector is shown in schematic form [16].

Also, [17], Research and applications that have been previously published are design, performance, heat transmission, experimental and numerical investigations, thermal heat storage, efficacy and compassion, and the most recent breakthroughs in this examination are addressed in this examination. It is reasonable to say that the energy analysis approach has been employed in many research despite the fact that the number of systems to which it has been applied is rather small. Solar air collector energy efficiency ranged from 47% to 89%, according to a study.

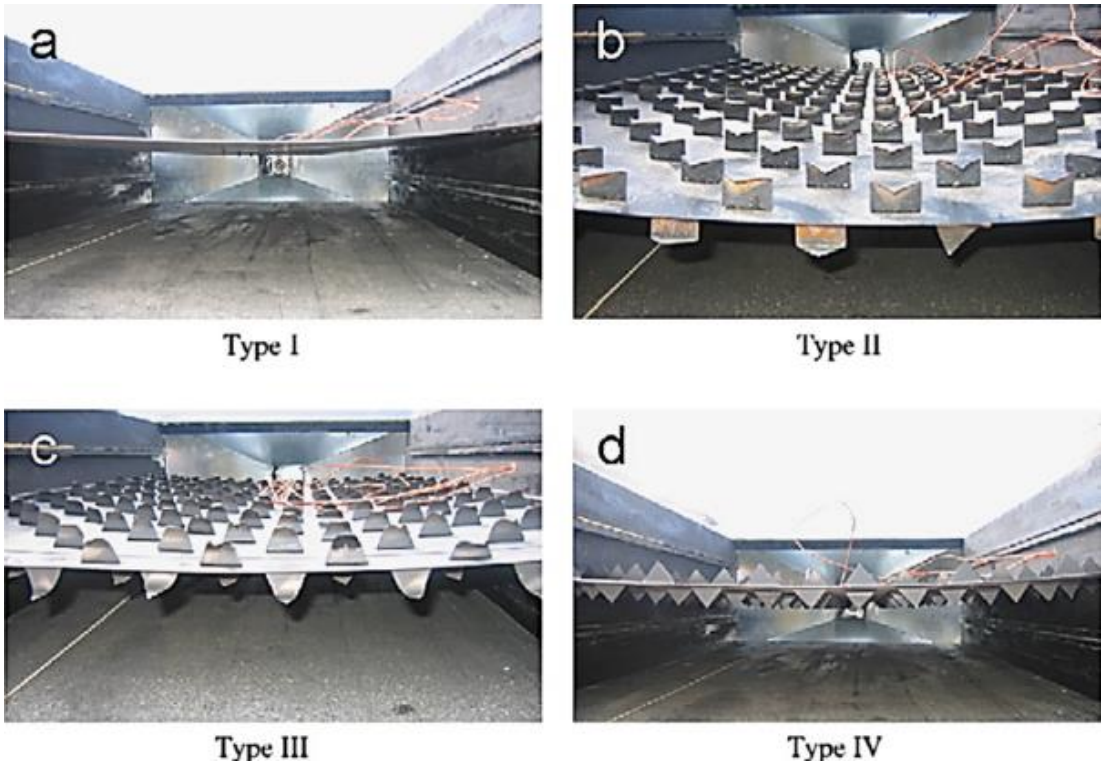

Figure 2.18. Four types of plates in solar air heater (a) type I, (b) type II, (c) type III, and (d) type IV [17].

In this study, [18], in order to boost the energy and energy performance, various absorber surface geometries are used in a second pass (roughened, finned, and v-corrugated wire mesh) is utilized (first pass). Solar air heaters of four types were tested in an experiment to determine their energy and exergy performance. Type-A was the v-corrugated wire mesh, Type-B was the finned plate, Type-C was the roughened plate, and Type-D was a single pass flat plate solar air heater, which is the standard. Comparing the outcomes was done (Type-D). These heaters were all designed and manufactured from scratch, and tested using an indoor experimental setup with varying mass flow rates and sun intensities. Mass flow rate promotes energy efficiency while decreasing air temperature rises. This research found that with a type-A solar air heater and a mass flow rate of only 0.01 kg/s, it was possible to raise the air temperature to as high as 26.28°C. Using solar air heaters of type, A, a flow rate of 0.04 kg/s results in an efficiency of 82,29%. With a bigger pressure drop and better exergy gain, Type-A solar air heaters are more efficient. Solar intensity (500–600 W/m^2) increases exergy gain, but energy efficiency remains practically same for all experimental circumstances when mass flow rate is maintained constant. Type-A solar air heaters

exceed the competitors in terms of efficiency and efficacy. The form of a solar air heater's surface has a considerable influence on its efficiency.

Figure 2.19. Photographic view of experimental setup [18].

In [19], The Completely Opposite Path Four transverse fins and wire mesh layers were used to manufacture and test the thermal efficiency of solar air heaters at Famagusta, Cyprus. It is replaced with sixteen layers of 0.18x0.18cm steel wire mesh with a diameter of 0.02cm, which is inserted into the absorber plate. There are three distinct sets of wire mesh layers, the first and second of which each include six layers, and the third of which only has four levels. In order to reduce the difference in pressure that develops between the layers in the duct, each group is partitioned off from the next by a wood frame that is 0.5 mm thick and runs perpendicular to the glass. Using an eight-letter route with a 3cm flow depth, the transverse fins propel air across the bed. On the other side, a large pressure drop is caused by the suggested design. Researchers found that when air mass flow rate rises from 0.001 to 0.03 kg/s, thermal efficiency improves. At a mass flow rate of 0.036kg/s, 65.6 % of the time, the system is at its most efficient. As AMF grows, T between AMF and TA declines. At 0.011 kg/s and a double pass, the output temperature difference was 43°C. Compared to a traditional solar air heater collector, thermal efficiency has risen.

In this experiment, [20] , Solar air heaters with improved air recycling are made using an absorbent plate that has been fitted with fins and baffles. Mathematical formulations and analytical research were used to design a recycles baffled double-pass solar air heater. Comparing theory and experiment It's a single-pass air heater, vs double-pass and recycling. The baffle-and-fin design enhanced heat transfer efficiency. Mass flow rate and recycle ratio affect heat-transfer efficiency and electricity consumption.

[21] Increase fluid velocity to enhance absorber-to-air heat transfer coefficient and collector efficiency. This concept employs aluminum cans as SAH absorber plates with flat, double-pass channels. Type I and Type II absorber plates utilized staggered cans. Third kind employs baffled flat plate (Type III). Double-passing is more efficient than single-passing for the same flow rate. Receiver fin efficiency was tested. Type II was more efficient than the other two versions. Wind speed promotes mass flow. Reduced heat transmission between the absorber and air lowers exit temperature.

In [22], Experimentation with a solar collector air in South Eastern European weather conditions yields results. For sun irradiation of 900-1000 W/m^2, it was proven that solar air collectors with baffles and a double air pass may achieve 50% efficiency in as little as 50 minutes. To enhance a building's natural ventilation, the researchers used a mathematical model and computational findings to size solar collectors for air transmission. Toward the end of the essay, a case study on how to size solar collectors for a two-story home or an office structure is included. In addition, the ACH coefficient was determined and compared to each other.

Figure 2.20. (a) Solar collector SH 1500, and system to modify the angle of inclination [22].

In this study [23] Solar air heaters with fins attached to an absorber plate have had their collector efficiency theoretically evaluated in a double-pass design. If the collector has fins and an external recycle is used, the collector's efficiency may be significantly improved. As a result of recycling, an increase in heat transfer coefficient has been achieved while a decrease in driving force temperature difference has been mitigated, resulting in an increased heat transfer area for the connected fins. Double pass with a recycle and fins are the rule of the day in devices of the same size. without fins, a double pass with a recycle without the need for a recycling or fins.

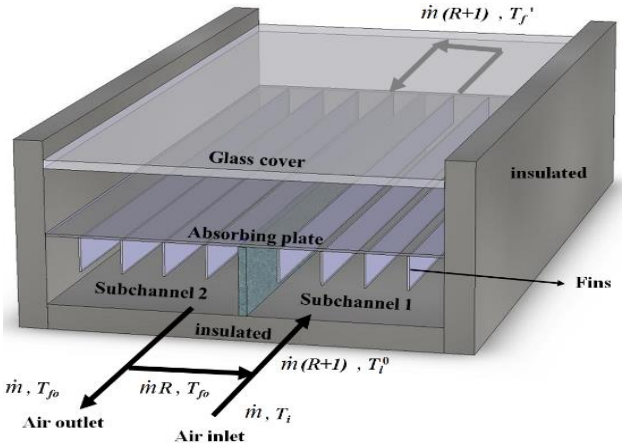

Figure 2.21. Schematic diagram of a downward-type double-pass external-recycle solar air heater with fins attached [23].

In this solar air heater [24], the flow area's heat transfer coefficient and air output temperature are increased by the fins. Collector efficiency also rises as a result. As a result, pressure losses and heat transmission have increased. In this experiment, the rectangular fins with two distinct surface areas are placed on the absorber in both free and fixed positions. This kind of absorber is made up of fins that may move freely on the absorber surface. Second, it has been bonded to the absorber surface. 1.642 m^2 of absorber surface area. The absorber's surface is covered by 8 and 32 fixed and free fins with 0.048 and 0.012 m^2 surface areas, respectively. Consequently, the overall fin area on the absorber surface has been calculated to be 0.384 units of area Comparing flat-plate solar air heaters to other solar air heaters and to free and fixed fin solar air heaters for efficiency and exergy loss ratio.

In this study [25] Mass flow rate, insolation, and flow channel depth affect collector energy, effective performance, and exergy. The present mathematical Model agrees with previous researchers' findings. Under similar operating conditions, corrugated absorber solar air heater performance is greatly increased with twin flow designs. At mass flow rates over 0.072 kg/s, all solar air heaters exhibit negative exergy efficiency. For all mass flow rates and insolation levels, the findings reveal that the AH-1 solar air heater's channel depth should be kept at or below 0.02 m for maximum efficiency. The performance suffers when the depth of the channel is increased or decreased by more than 0.2 m.

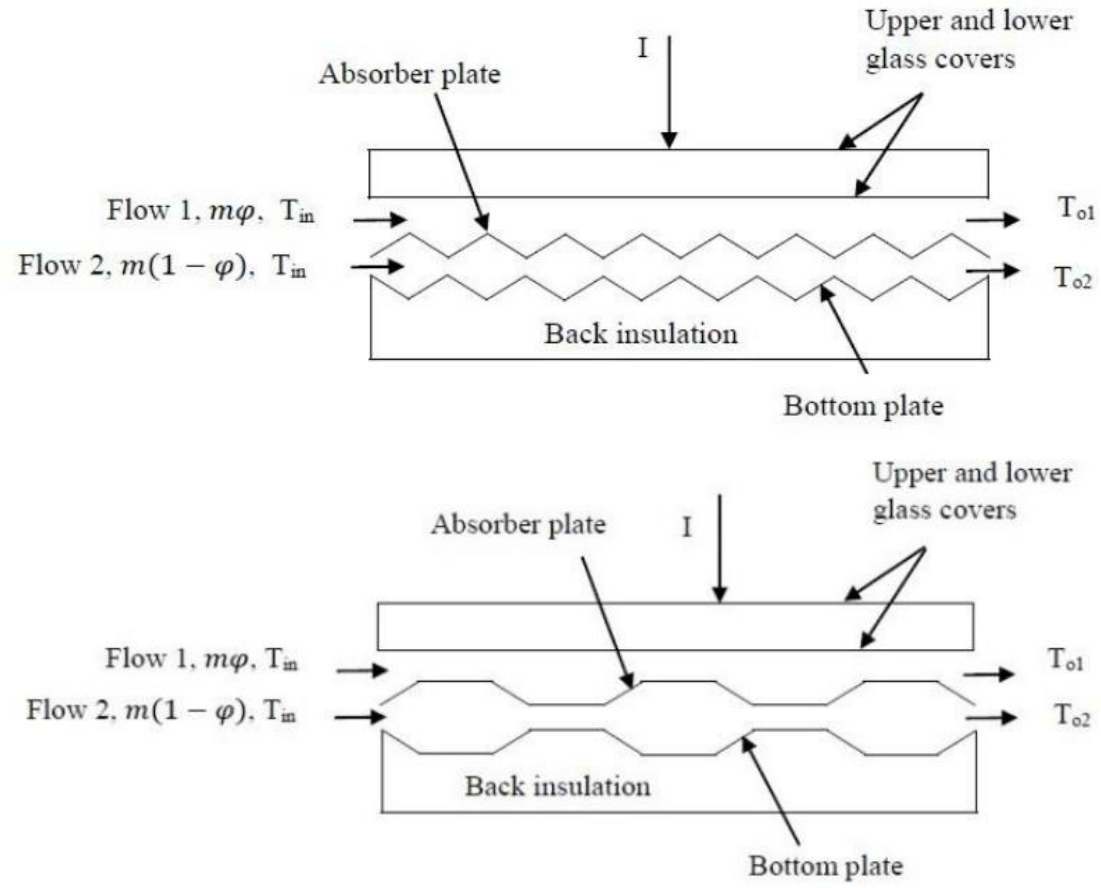

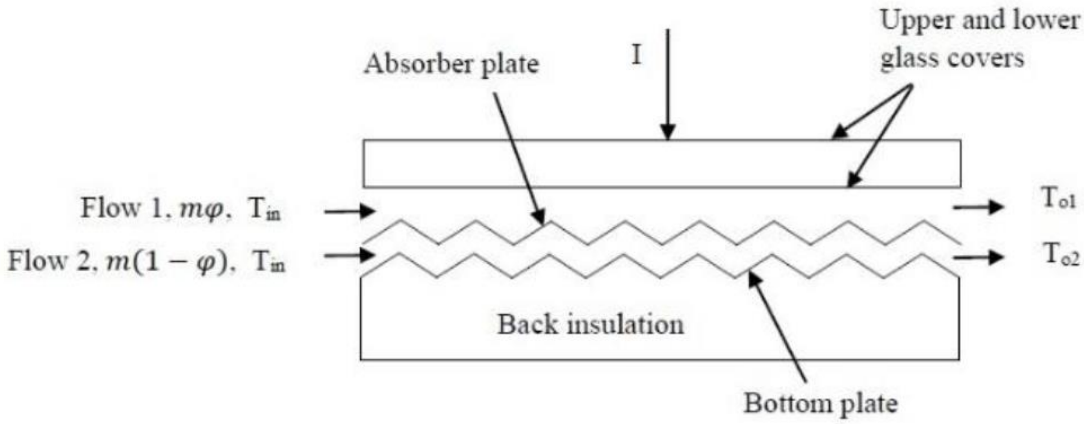

Upper and lower glass covers
Absorber plate
I
Flow 1, $m\varphi$, T_{in}
Flow 2, $m(1-\varphi)$, T_{in}
T_{o1}
T_{o2}
Back insulation
Bottom plate

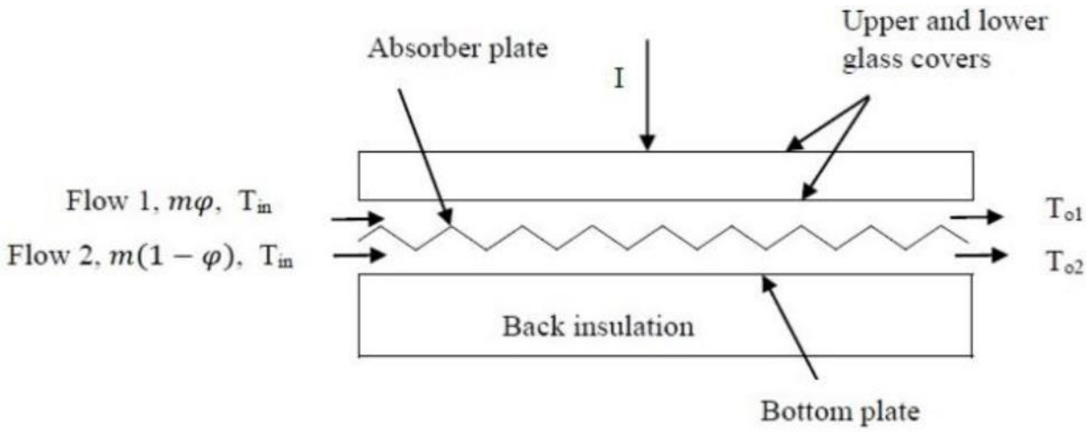

Upper and lower glass covers
Absorber plate
I
Flow 1, $m\varphi$, T_{in}
Flow 2, $m(1-\varphi)$, T_{in}
T_{o1}
T_{o2}
Back insulation
Bottom plate

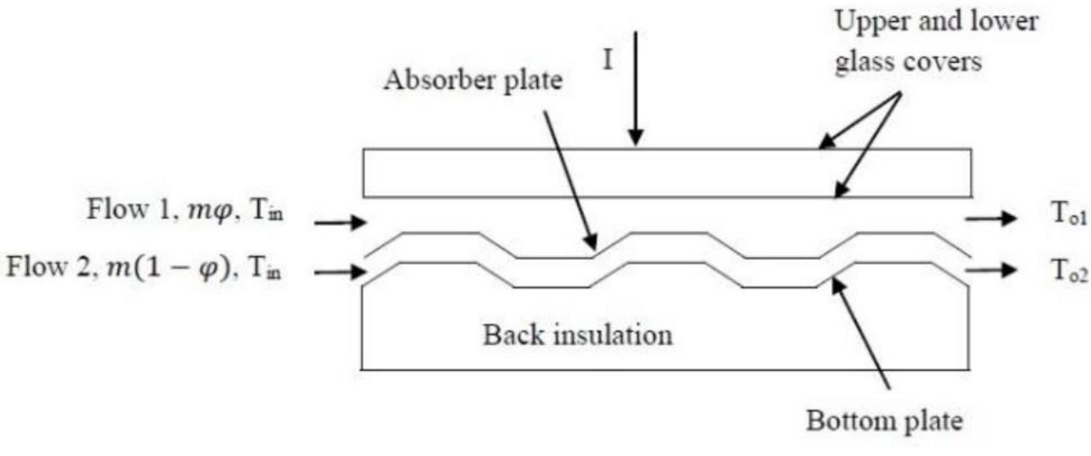

Upper and lower glass covers
Absorber plate
I
Flow 1, $m\varphi$, T_{in}
Flow 2, $m(1-\varphi)$, T_{in}
T_{o1}
T_{o2}
Back insulation
Bottom plate

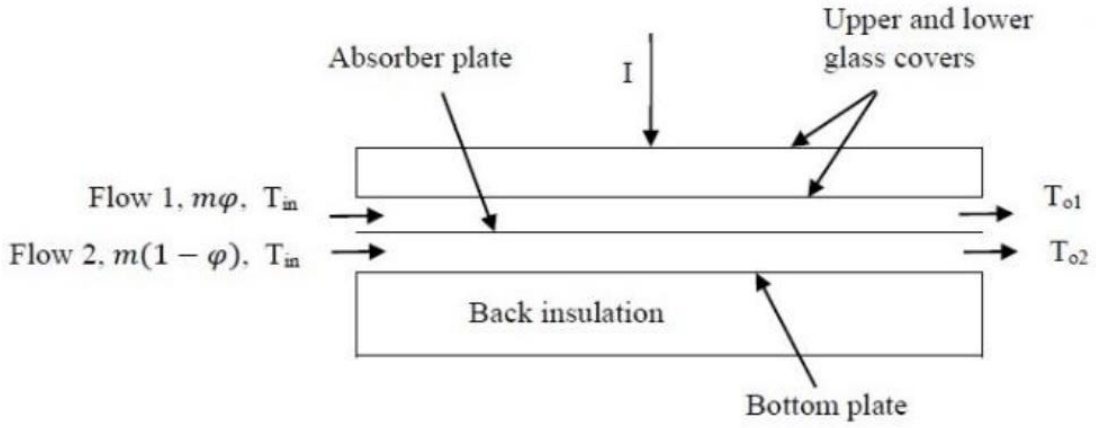

Figure 2.22. The double flow type solar air heaters for different design of absorbing plates [25].

An experimental study has been performed in [26] Solar air collectors with porous obstructions of varying thicknesses on flat plates, as well as collectors with no impediments at all will be analyzed for their energy consumption (flat plate). Aluminum foams are utilized as a porous material. The SACs covers have them arranged in a staggered fashion so that they appear consecutively. Two distinct air mass flowrates, 0.016 kg/s and 0.025 kg/s, and two different thicknesses, 6 mm and 10 mm, are tested. The first law of thermodynamics is used to determine the energy efficiency of SACs. When it comes to solar air collectors, a comparison is done between five different models and their energy efficiency. It was discovered that SACs with a thickness of 6 mm and a mass flow rate of 0.025 kg/s had the highest collector efficiency as well as an increase in air temperature.

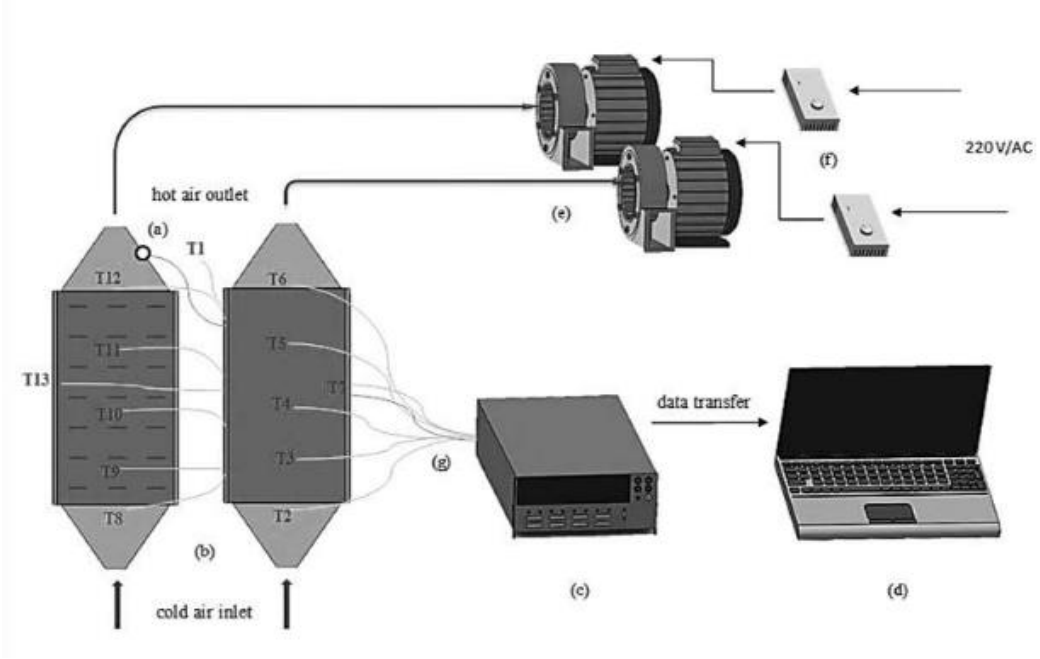

Figure 2.23. Schematic view of experimental set-up. (a) pyranometer, (b) solar air collectors, (c) data logger, (d) computer, (e) radial fans, (f) velocity control devices, (g) thermocouples [26].

Instead of a flat absorber, an experiment was conducted using aluminum mesh wire to examine the thermal performance of a double pass solar air heater [27]. boosting both the airflow and the heat transfer coefficient between the absorber plate and the surrounding air and the air may bring about an improvement in the collector's overall efficiency. Wire mesh in both the bottom and top channels has also been studied as a factor in the study's findings. Solar air heaters that use square wire mesh have a higher output temperature, which boosts thermal efficiency and indicates great potential to heat air in both types of solar air heaters, as shown by the experiment. MSAH, a solar air heater using aluminum mesh wire, has been found to function pretty well compared to traditional solar heaters in terms of heating air (CSAH). The largest temperature differential that was measured using an aluminum mesh wire matrix absorber was estimated to be 31°C at a mass flow rate of 0.00527 kg/s. This was 19% greater than usual. Aluminum mesh solar air heaters have the highest thermal efficiency and mass flow rate. 14–19% more efficient than solar heaters. High-flow solar heaters are more efficient. Solar air heater efficiency increases with airflow. Exhaust air temperature lowers as mass flow rate rises. Aluminum mesh wire matrix absorbers increase heat collection and transfer. 10°C separates ambient and input air. The aluminum mesh wire

matrix absorber solar air heater reached 62°C, whereas a standard one only reached 44°C.

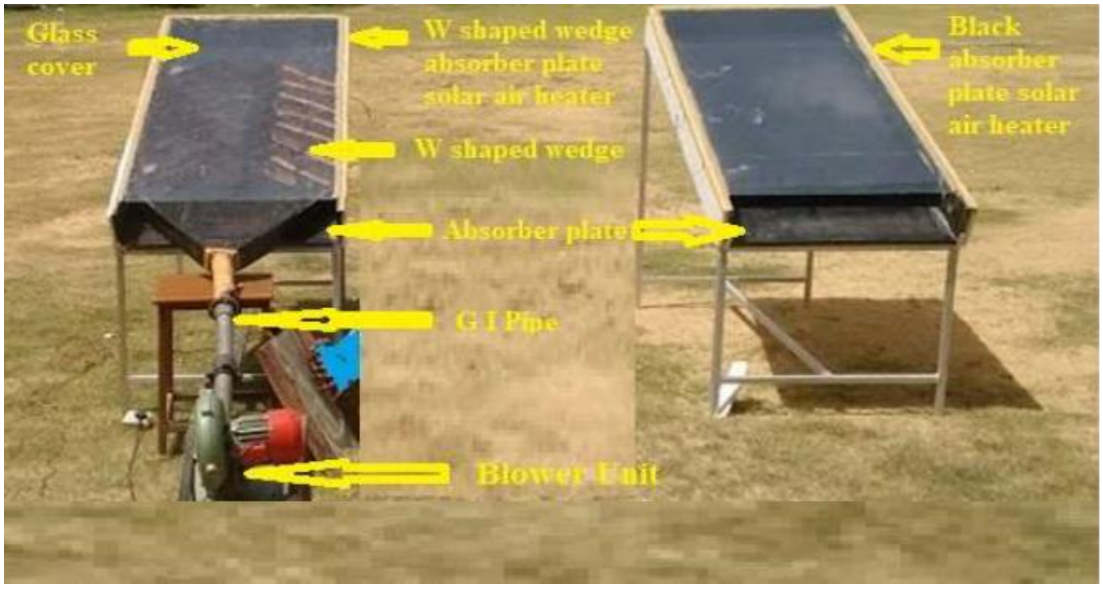

Figure 2.24. Pictorial view of experimental setup [27].

Solar Air heaters may look better with ribs above the absorber plate. Turbulence increases heat transfer and friction factor [28]. Multiple studies demonstrate that double pass sun air heaters are more thermally efficient than single pass models. Distinct ribs above the absorber plate promote heat transfer. This paper describes artificial roughness added to the absorber plate to increase turbulence. This research summarizes single and double pass solar air heaters' thermal and thermos hydraulic efficiencies, Nusselt Numbers, and Friction Factors. Comparable absorber plate designs are more efficient in heating solar air than one pass versions. Distinct ribs above the absorber plate transmit heat better than continuous ribs. Double-pass solar air heaters may attain 80% thermal efficiency using a fin or wire mesh structure.

Air mass flow affects collector thermal performance and pressure decreases [29]. Flat-plate solar air heater thermal efficiency is being studied. Temperatures of the absorbent plate, input and output, and surrounding air were monitored. Flow channel duct air mass flow rates were also tested. Smooth-plate second-pass solar air heaters increase efficiency by 3-4 %. Porous media solar air heaters are 5% more efficient than single-pass models, whereas double-pass devices without media are 3% to 5% more efficient. Experiments are utilized to explore how different factors affect how solar air heaters

with or without a porous medium perform in terms of thermal performance and pressure decrease. The thermal efficiency research found that mass flow rate affects pressure drop.

Figure 2.25. Experimental Set-up [29].

[30] A double-pass solar air collector was tested for performance. For double pass solar air collectors, a better thermal efficiency may be achieved by utilizing a porous material in the second pass of the absorber matrix. Porous materials are ideal for heat transmission because they have a wide surface area. More than a quarter of a percent better thermal performance was seen in double-pass solar air collectors made from porous materials than those made without porous materials.

In the other hand, [31], in order to evaluate the thermal performance of a flat plate solar air heater, tests were conducted in a laboratory-sized setup with a constant solar radiation intensity of 600W/m^2 and a 30° tilt. Flat-plate solar air heaters tilted at 30° and subjected to a constant solar radiation intensity of 600 W/m^2 were evaluated for their thermal performance in a laboratory-scale test cell. One-meter by five-meter-by-0.1-meter solar air heater is presently functioning after the design and production process. Natural convection and forced convection were both found to work as predicted for the plane absorber (basic design), When used in a forced convection setup, inclined V-porous ribs with conducting side walls performed similarly to those with straight side walls. All of the testing was done in an artificially lit setting.

Different designs of the solar air heater's input ports were examined for their thermal efficiency and temperature gradient in normal to the base of 31cm.

2.5. SUMMARY

There are several researches focusing on various elements of the double pass solar air collectors, such as the impact of the number of passes, the kind of extended surface, design and material used to build the absorber plate. Few researches have focused on the use of recycled cans as an additional surface area for recycling. The position of the cans on the absorber plate has been found to have a major impact on thermal efficiency, therefore this research evaluated two distinct orientations. Using open access literature, the author believes that there is inadequate research that examine the influence of expanded surfaces (fins) on the performance of double-pass solar air collectors. For the most part, this research aims to fill in the information vacuum around Double-Pass Solar Air Collectors (DPSAC). Extended surfaces (such as hollow cans) with varying forms and orientations on the absorber plate are examined in this research.

PART 3

METHODOLOGY

3.1. INTRODUCTION

This chapter explains the required procedure to accomplish the whole study as well as the current experimental work. The beginning as depicted in Figure 3.1 was with the literature survey, where related previous studies were discussed in chapter 2.

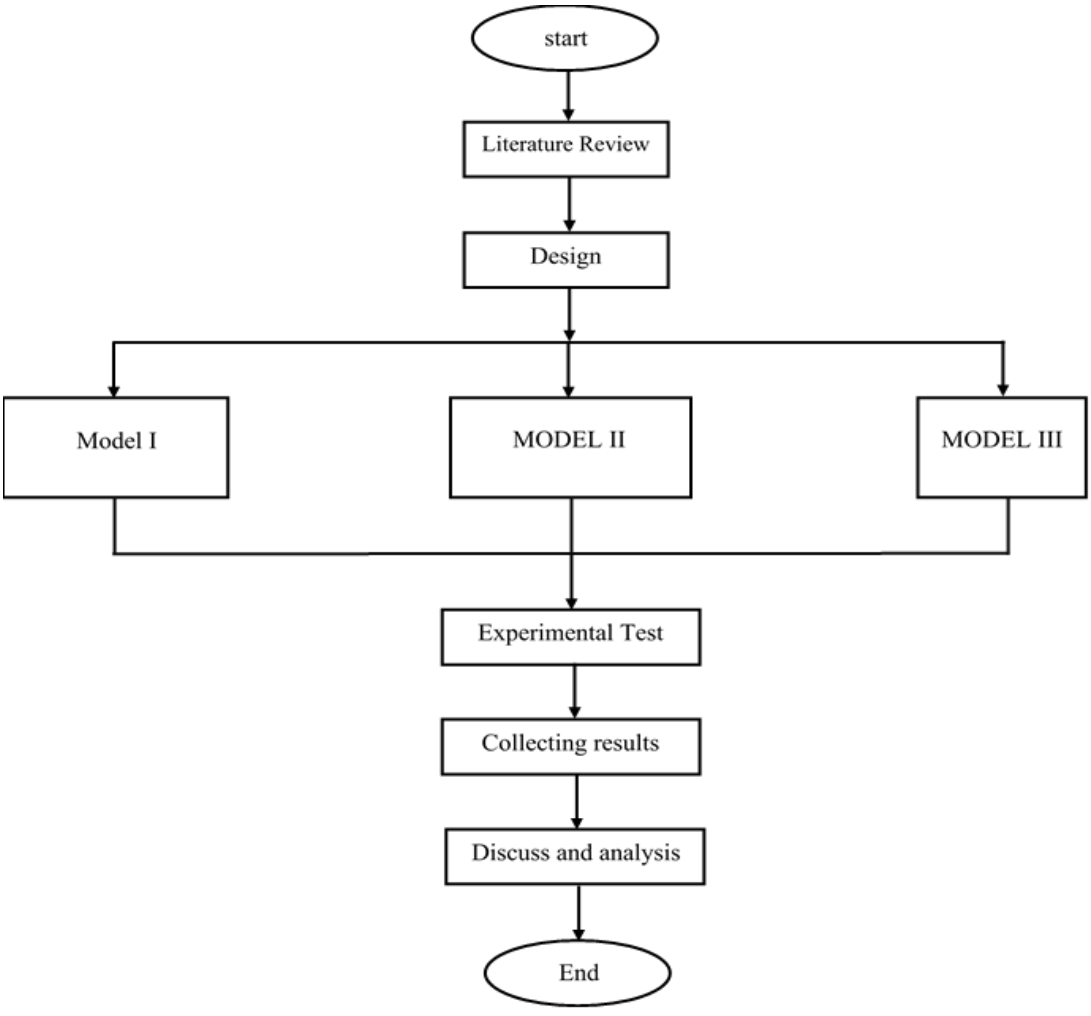

Figure 3.1. Flow chart of the study.

Via surveyed literature, two Models were modified for the absorber plate along with flat absorber plate, Model I, Model II, and Model III which will be discussed next. Moreover, in the experiment test stage, the method of making each model is described in detail besides the technique followed in collecting results. Finally, the collected results discussed and analyzed and presented in different forms such as thermal efficiency in teams of solar radiation and mass flow rate as well as can orientations on the absorber plate.

3.2. REQUIRED TOOLS AND INSTRUMENTS

In this section each of the essential tools and instruments which have been utilized in this study are described. The following sections define each of them:

3.2.1. Wood Frame Box

For the DPSAC, three variants were created, each having a different absorber plate but the same overall dimensions. For the collector's bases and sides, plywood with a thickness of 2 cm was utilized (k= 0.13 W/m.k). Plywood is a heat insulator, but Perspex was used to cover the collector's upper portion, allowing solar radiation to flow through while preventing heat from escaping.

Figure 3.2. The wood frame of the DPSAC.

A sheet of Perspex with a thickness of 4 mm was employed. It was 122 cm long, 60 cm wide, and 15 cm high 25 cm. An upper and lower base of 60 cm (and 14 cm, respectively) separate the collector's trapezoidal form, which is 22 cm in length, from the collector's rectangular shape, which measures 100 cm (and 60 cm). The collector wood frame is seen in Figure 3.2. In order to maximize absorptivity and prevent heat loss, the whole collector was painted black. Upper and lower collection channels are separated by the absorber plate. The last channel sections of both channels are also the same height and trapezoidal shape. It must be remarked that each wood frame has two pipes with diameter of (48mm) located on the trapezoidal section, which was utilized for inlet and outlet air as depicted in Figure 3.3.

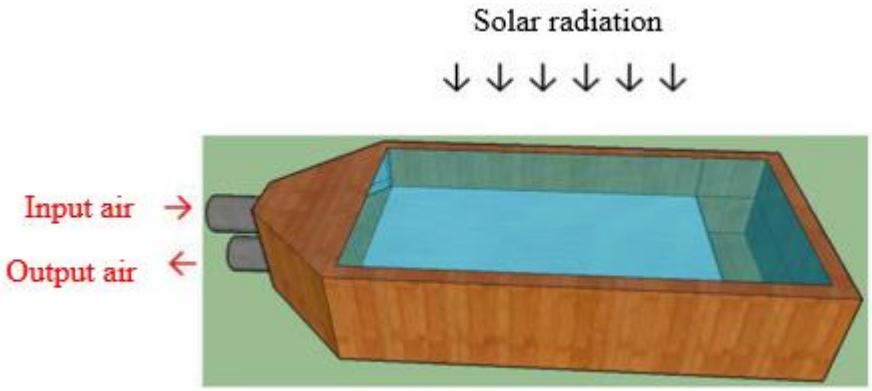

Figure 3.3. The examined DPSAH.

Figure 3.4. Iron stand frame

The solar collector was mounted on iron frame stand, which helps to control, rotate, and move the SAHC easily as shown in Figure 3.4. The final shape of the wood frame box after painting and mounted on the iron frame is shown in Figure 3.5.

Figure 3.5. Final shape of wood frame box.

3.2.2. Absorber Plate

As previously stated, this research tested three different kinds of absorber plates, each of which was manufactured of aluminum with a thickness of (1mm). In order to maintain a high absorbance, the absorber plate was (85 cm x 56cm) and painted black. Using an absorber plate positioned 12.5 cm away from the collector base, we created an empty space 15 cm long so that air could be pushed to go from the upper channel to the lower channel and leave the collector. In this way, it is referred to as a two-stage collector. Recycled cans on the absorber plate can be oriented in three different ways, hence three different designs were created. In the absorber plates, an aluminum plate was employed because of its high thermal conductivity k=217 W/m.k and high absorptivity 0.94, both at 100 °C 0.09 (Rohsenow et al., 1998).

The first model of the absorber plates was flat Figure 3.6 (a), where no recycled cans fixed on it. The advantage of utilizing this model is to compare with the other models. In the other hand, the second model was flat plate with cans distributed in zigzag orientation as shown in Figure 3.6 (b).

(a) (b)

Figure 3.6. Examined absorber plate models: (a) model I, and (b) Model II.

Furthermore, longitudinal and transverse cans distributed alternatively in both horizontal and vertical directions. It should be noted that two types of recycled cans were fixed on the absorber plate, longitudinal and transverse cans, Table 3.1 clarifies the dimensions of the utilized recycled cans.

Table 3.1. Types of utilized recycled cans

Can type	**Length (mm)**	**dimeter (mm)**
Longitudinal	130	50
Transverse	90	70

Finally, the third model III, both types of recycled cans were used to form alternative columns. Moreover, longitudinal cans fixed first on the upper left side, then transverse cans fixed as shown in Figure 3.7.

Figure 3.7. Model III

3.2.3. Blower

Blower fan was used to provide air to the system. The technical descriptions of the utilized blower were 2 inches, 150 W,3600 R.P.M,v=10-18 m/s, the blower was mounted at the entry of the collector by the connected pipe among them and air speed was regulated by a side guide's vanes, Figure 3.8 displays the blower used in this work.

Figure 3.8. Blower used in the present work.

3.2.4. Thermocouples

During the testing, the thermocouple wire of the (k) type was used to record the temperatures. This type of thermocouple can measure temperature up to 400 ℃ with accuracy ± 2.5 ℃, the utilized type is displayed in Figure 3.9.

Figure 3.9. Thermocouple ustilted in the present work.

When attaching the thermocouple wires to the absorber plates, great care was taken to avoid damaging them. In order to protect each on thermocouple, an aluminum shelter encased in adhesive tape was attached to each one. The aluminum lining prevents direct exposure to solar radiation and helps to make the thermocouple measures the temperature of the absorber plate precisely. Four thermocouples measure the absorber plate's temperature. In each model, these thermocouples were mounted at the absorber plate's middle (20 cm). Totally five thermocouples were positioned on each model, four on the absorber plate Figure (3.10a) and the fifth one located on the back of the wood frame box to measure the output temperature Figure (3.10b). In all, fifteen thermocouples were employed for this experiment, and each one was connected to a selector switch (which will be covered in the next paragraph).

(a)

(b)

Figure 3.10. Thermocouples fixed on the absorber plate.

3.2.5. Selector Switch

The temperature measurements at different positions on the absorber plate performed using a selector switch. Selector switch model (AZUN 96), (max 24 V, max 200 mA) was used to link the thermocouples with digital controllers which explained next. This device contains (24) channels and it can be connected (24) to thermocouples. This device receives a signal from the thermocouple and converted to the digital controller. It can convert the reading from one thermocouple to another by moving the selector from channel to another. Figure 3.11 shows the utilized selector switch in this work.

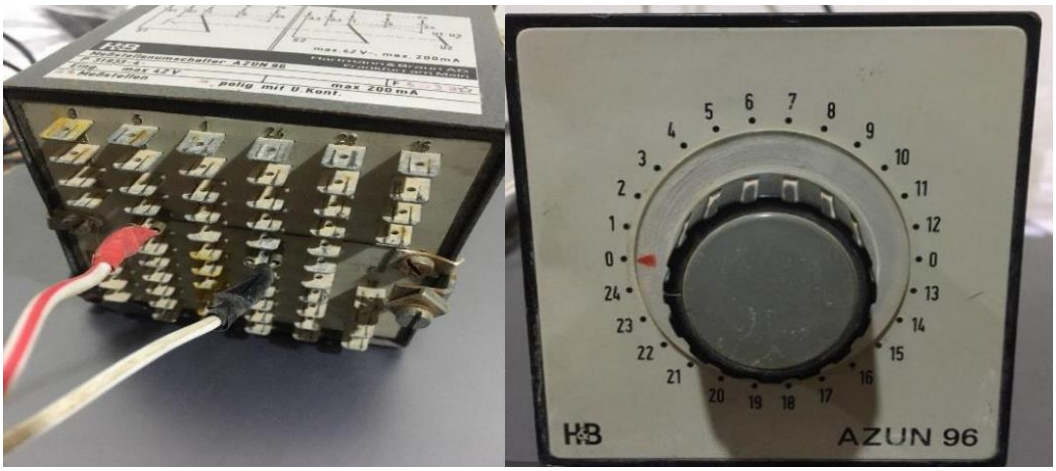

Figure 3.11. Utilized selector switch.

3.2.6. Digital Controller

Digital Controller model of (TA10 –INR), Input (TC/RTD), Output (4-20mA), (Accuracy: ±0.3 % F.s), (power:90-260 V AC/DC) was used to display measured temperature, Figure 3.12. It receives the signal from the selector switch and converts to the digital screen that can be read. This numbers represent the measured temperature by the thermocouple.

Figure 3.12. Digital controller.

3.2.7. Anemometer (Hot Wire)

An anemometer is a device that measures the speed of the air. (TES 1341) type was used in the tests to determine air velocity at entering and leaving in the collector, Figure 3.13. A hole was made in the two tubes fixed on the inlet and outlet of the collector. This hole is used to access the hot wire to measure air velocity at the inlet and outlet from the collector.

Figure 3.13. Hot wire device.

3.2.8. Thermal Camera

Thermal camera is used to take a photo for the temperature distribution on along the absorber plate. This device model is (FLIR E5). This camera was used to take thermal pictures for the absorber plate, so that shows the temperatures on the absorber plate surface and determines the highest temperature on it, Figure 3.14 displays the thermal camera.

Figure 3.14. Thermal camera.

3.2.9. Solar Power Meter

A solar meter is used to measure the sun's radiance. Figure 3.15 shows the absolute inaccuracy for this particular device model (SP-216): 2%. It was used to measure solar radiation during the days that the experiment was conducted. The meter measures the total solar radiation per unit area (W/m^2) of the collector surface.

Figure 3.15. Solar power meter.

3.3. EXPERIMENT PROCEDURE

There are different steps should be taken before each test. These steps are summarized as follows:

- Cleaning the perpex covers.
- Checking the thermocouple junctions and their attachment on the surfaces.
- Checking the equilibrium of manometer fluid.

It should be noted that the angle of inclination of all collectors are the same. It is appropriate to make all models work at the same time for the sake of comparison. The process of experimental procedure includes the following steps:

1) Lifting the cover of all collectors and sure, the glass transparent is clean from dust and humidity.
2) Choosing the air blower slot with the lowest discharge and running the blower at the time 08:30 AM. This is done to make sure that there is no leakage from collectors and be sure that the instruments measure right day.
3) Starting recording the readings at 9:00 AM for each of the following:

    a) Recording air velocity at the entry and exit from the collectors.

b) Recording temperatures at the entry and exit from the collectors, temperature of collectors, and temperatures on absorber plates.
c) Recording solar intensity.
d) Recording the external weather conditions.

4) Re-registration of data every half an hour with the need to take into consideration the external weather conditions.
5) Ending readings recording at (04:00 PM) and ensure that all collectors are covered to maintain from dust and moisture.

3.4. PRESSURE DROP

Pressure drop is a critical factor to consider when evaluating the efficiency of solar collectors. To calculate the pressure, drop the following analysis will be followed, total pressure drop across the double pass solar heater collector will be calculated as [21,32]:

$$\Delta p = \Delta pf + \Delta pother \tag{3.1}$$

Where Δpf represents pressure drop due to friction losses, which may be represented from following equation:

$$\Delta p = \frac{\rho}{2} . f . \frac{v^2}{D_h} . L \tag{3.2}$$

Where f is friction factor which is calculated depending on the Reynolds number.

$$f = \frac{0.316}{Re^{0.25}} \tag{3.3}$$

$\Delta \boldsymbol{P}$ other represents pressure drop due to minor losses through the collector [33].

$$\Delta p_{other} = \frac{1}{2} . k_L . \rho . v^2 \tag{3.4}$$

Where $K_L = K_{exit} + K_{entrance} + K_{bend}$

These values are taken as (0.5, 1, and 2.2) respectively [36]. Reynold number can be calculated from the following equation [34]:

$$Re = \frac{\rho . v . D_n}{\mu} \tag{3.5}$$

Where ρ and μ are calculated based on the equations below [35, 36] :

$$\rho = \left(\frac{353.04}{T_{ave} + 273}\right) \tag{3.6}$$

$$\mu = \frac{(0.000001458) * (T_{ave} + 273)^{1.5}}{T_{ave} + 384.4} \tag{3.7}$$

(D_h) represents hydraulic diameter of the duct which is calculated as $D_h = 4A/P$ [36],

where:

T_{ave}: average temperature $T_{ave} = (T_{in} + T_{out})/2$

A= cross sectional of duct A=b*h

P= perimeter of the duct P=2(b+h)

L: length of collector (m)

h: height of collector (m)

b: width of collector (m)

ρ: density (kg/m^3)

Re: Reynold number

μ: dynamic viscosity (kg/m.s)

v: the measured air velocity at the collector inlet pipe (m/s)

3.5. CALCULATIONS

3.5.1. Energy analysis

The useful heat gain (Q_u) is given by [38]:

$$Qu = \dot{m}\, CP\, \Delta T \tag{3.8}$$

$$\Delta T = (T_{out} - T_{in})$$

C_p = specific heat (J/kg. °C)

$$C_p = 1.0057 + 0.000066(T_{ave} - 27) \tag{3.9}$$

The air mass flow rate (ṁ) is given by [39,40]:

$$\dot{m} = \rho\, A\, V \tag{3.10}$$

Where:

A = Cross sectional area of duct (m^2).

The thermal efficiency of the heater, denoted by (η_{th}), is defined as the ratio of the rate at which useable heat is gained by the air passing through the heater to the amount of solar energy that is incident on the heater surface [41,42]

$$\eta_{th} = \frac{Q_u}{I\, A_b} \tag{3.11}$$

$$Daily\ efficiency \quad \eta_{th}\% = \frac{\sum Q_u}{\sum I A_b} \tag{3.12}$$

where: A_b = the area of absorber plate (m^2).
I = the total amount of solar energy that strikes the heater (W/m^2).

3.5.2. Thermocouples Calibration

All equipment used in measurement was calibrated to ensure that the utilized equipment is good and ready to use. The thermocouples were checked before they fixed in their positions, for accuracy and precision. The check was achieved by

immersion in a water bath and checking the temperature against a mercury_ glass thermometer, be the uncertainty was ± 0.2°C. The temperature of the water varied from an approximately 0°C (ice bath) to just under 100 °C in (10-15) °C. The water was stirred between the temperature levels to overcome the nonuniform in water temperature. All thermocouples had the precision of ± 0.2 °C.

3.5.3. Uncertainty Analysis

It messes with each measured parameter by its own uncertainty and adds up all the messes for a worst-case scenario. The findings of the elemental uncertainties measurements from various studies are presented in Tables 3.2 and 3.3. These tables include the results of the various experiments.

Table 3.2. Utilized equipment precision [42] [43].

Equipment	Range	Resolution	Accuracy
Thermocouple type K	-270 to 1260 °C	1 °C	±2.5°C
Pyrometer	0-2000 W/m^2	æ	±5 W/m^2
Thermal anemometer	0-20 m/s	0.01 m/s	±0.03 m/s

Table 3.3. The uncertainty values in measurement and calculation [44].

Parameter	Uncertainty
Temperature	±1.4°C
Solar radiation	± 5 W/m^2
Mass flow rate	± 0.002 kg/s
Thermal efficiency	± 4%
Exergy	± 5%
Exegetic efficiency	± 3%

PART 4

RESULTS AND DISCUSSIONS

4.1. PREFACE

The readings recorded in February and March were analyzed and the factors affecting the performance of the solar air heater were calculated clarified and discussed in this chapter. In order to reach certainty of the results and to obtain reliability in the laboratory-made practical system, some results of the practical side were compared with previous studies. In order to know the best arrangement of the changes made to the solar air heater, a comparison made between the three collectors under different working conditions. As previously stated, the trials were conducted at Ramadi, Anbar Governorate, Iraq, which is located at 43.268° east longitude and 33.43° north latitude, at an elevation of 59.8 m above sea level. The city of Ramadi is known for having a high amount of sun radiation throughout the year. Also, the rate of solar radiation for the winter months is us full for heating and drying agricultural crops. The solar radiation rate for the winter months' ranges from 3000 W/m^2 in November to 4300 W/m^2 in March. Figure 4.1 shows the daily solar irradiation of Ramadi city. It's clear that the amount of solar irradiation is good enough for use in heating and drying applications of agricultural crops. The operating time of the three systems starts from nine in the morning until four in the afternoon. The three solar collectors are oriented southward and tilted at an angle of 45° in order to ensure that the collectors are almost opaque with the solar radiation most of the time. The experiments were conducted for fifteen days, and only the results of the clear days considered.

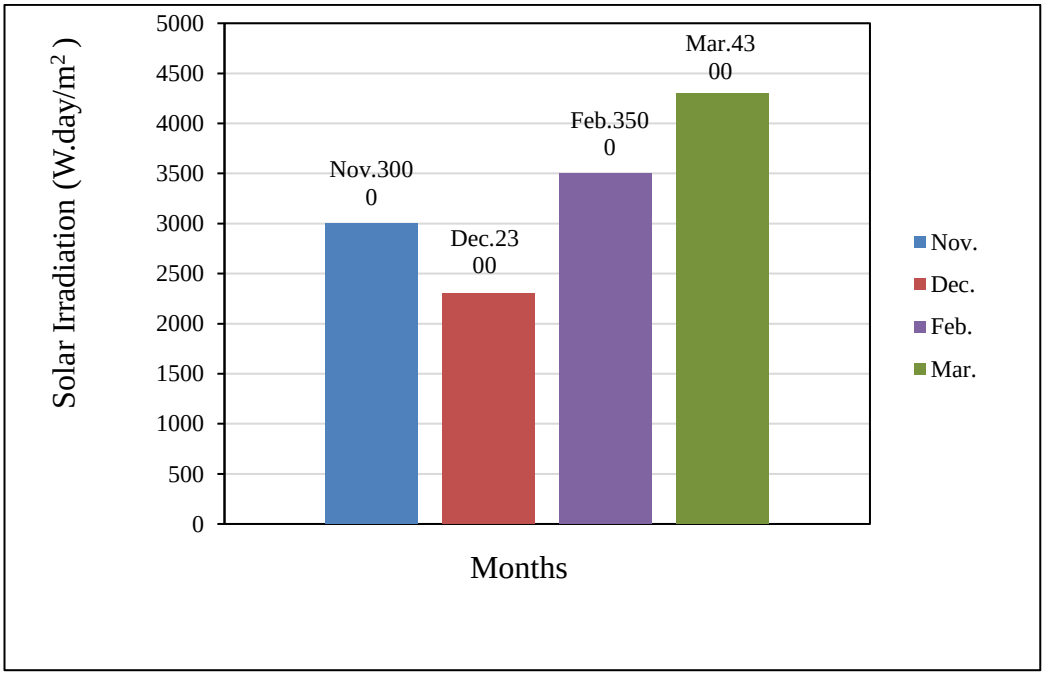

Figure 4.1. Diagram showing heat radiation with months February and March for 2022.

4.2. PRELIMINARY VALIDATION OF TEMPERATURE MEASUREMENTS

To guarantee the trustworthiness of the data regarding the thermal performance of the solar collectors, the thermocouples were correctly installed on the absorbing plate of each collector utilized in the studies and that the reading of these thermocouples is correct, a thermal camera has been relied upon to give a temperature distribution on the absorber plate. Figure 4.2 shows images taken using the thermal camera for the three collectors. When comparing the temperature ranges shown in the image, we noticed that the thermocouple readings are very close to them.

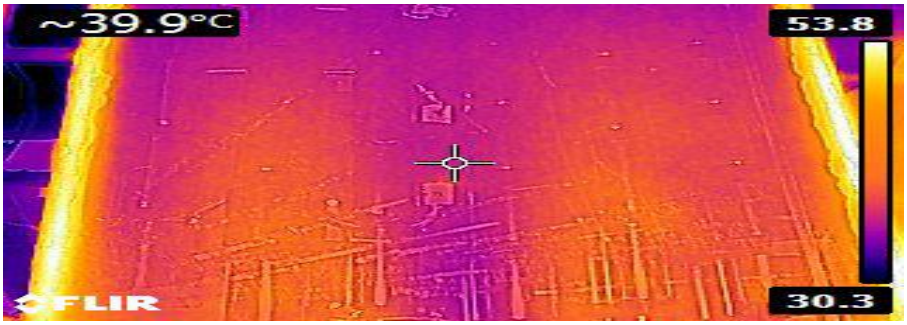

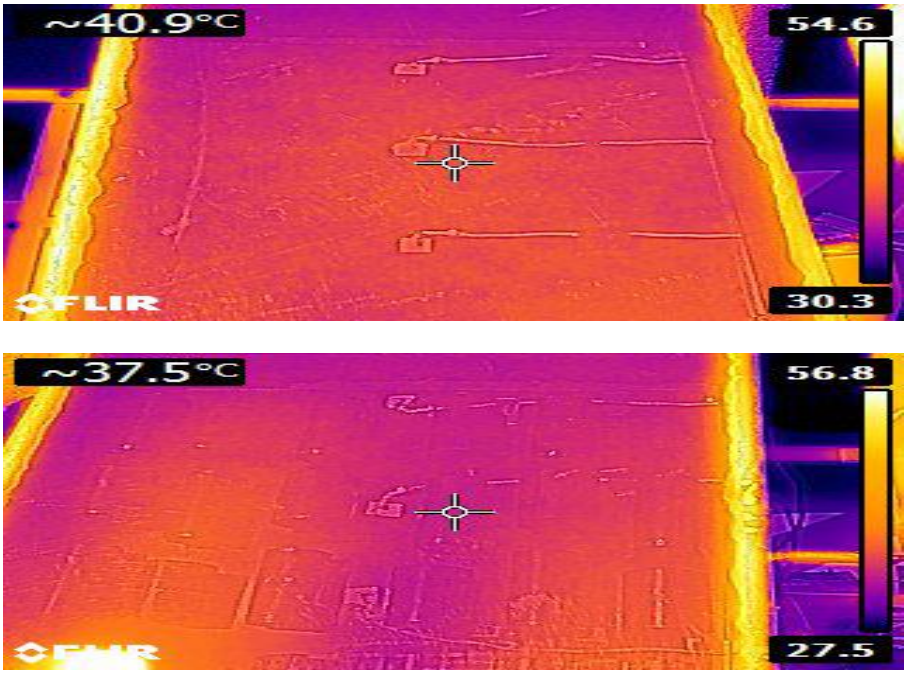

Figure 4.2. The pictures of absorber plates with three models that taken by the thermal camera.

4.2. COMPARISON WITH PREVIOUS WORKS

4.2.1. Comparison of Thermal Efficiency

The steps that are adopted for the manufacture of practical systems for conducting experiments on the issue of solar air heaters have been approved by ASHREA standards. For the reliability of the systems used in the current research, a comparison was made between some of the results of the current research with previously published research. Figure 4.3 shows a comparison of the thermal efficiency with time with the results of [45]. It's clear that the results of the present study are very closed to that of the previous published results. The exergy efficiency from the second law of thermodynamics equals:

$$\eta_{EX} = \frac{EX_{air}}{EX_{collector}} = \frac{\dot{m}(\Delta h - T_{\infty}\Delta S)}{\alpha.\tau.I.A_c\left(1 - \frac{T_{\infty}}{T_s}\right)} \quad (4.1)$$

Where:

EX_{air}: exergy of air (J/s).

$\dot{m}$: mass flow rate of air (kg/s).

Δh: change in enthalpy (J/kg).

ΔS: change in entropy (J/kg.k).

$EX_{collector}$: exergy of collector (J/s).

α: absorption of an absorber plate.

τ: transmittance of glass cover.

I: solar radiation (W/m^2).

A_c: collector surface area (m^2).

T_∞: environmental air temperature (K).

T: air temperature

s: entropy (J/kg.k).

εg: glass emittance

εp: plate emittance (0.96)

σ: the Stefan-Boltzmann constant (5.67× 10^{-8}W/m^2.k).

αp: the absorber plate absorptivity (0.94-0.97).

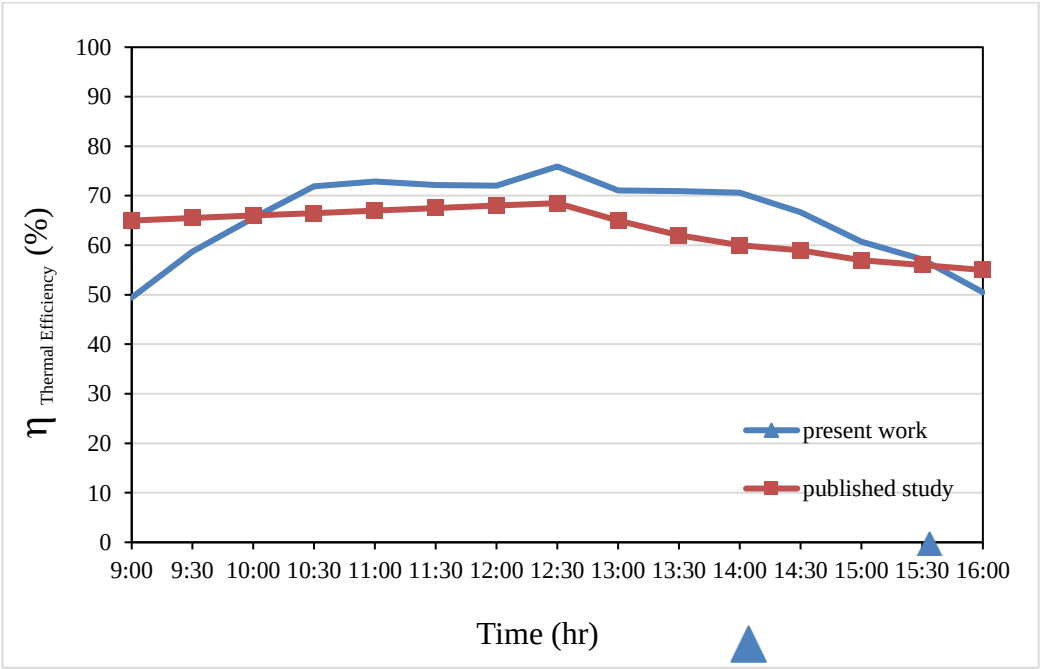

Figure 4.3.Thermal effciency variation with time. Model II for the ṁ=0.026 kg/s on Wednesday (23/2/2022).

4.2.1. Comparison of Second Law Efficiency

Efficient thermodynamic systems are characterized by their exegetic efficiency, which may be calculated by determining how much energy a system produces and how much energy it receives. Figure 4.4 shows a comparison of the exegetic efficiency from the preset work with that of Farhan, A. and his friends [46]. It can be seen that the behavior is very close throughout the time of the experiments and the difference is caused due to the difference in the solar irradiation values and the shape of the solar collector used. The thermal efficiency of the solar air collector (η):

$$\eta = \frac{Q_u}{A_c Q_{inc}} \tag{4.2}$$

Where:

η: thermal efficiency

Q_u: useful gained thermal energy (W/m^2).

A_c: the collector upper surface area (m^2).

Q_{inc}: incident solar radiation (W/m^2).

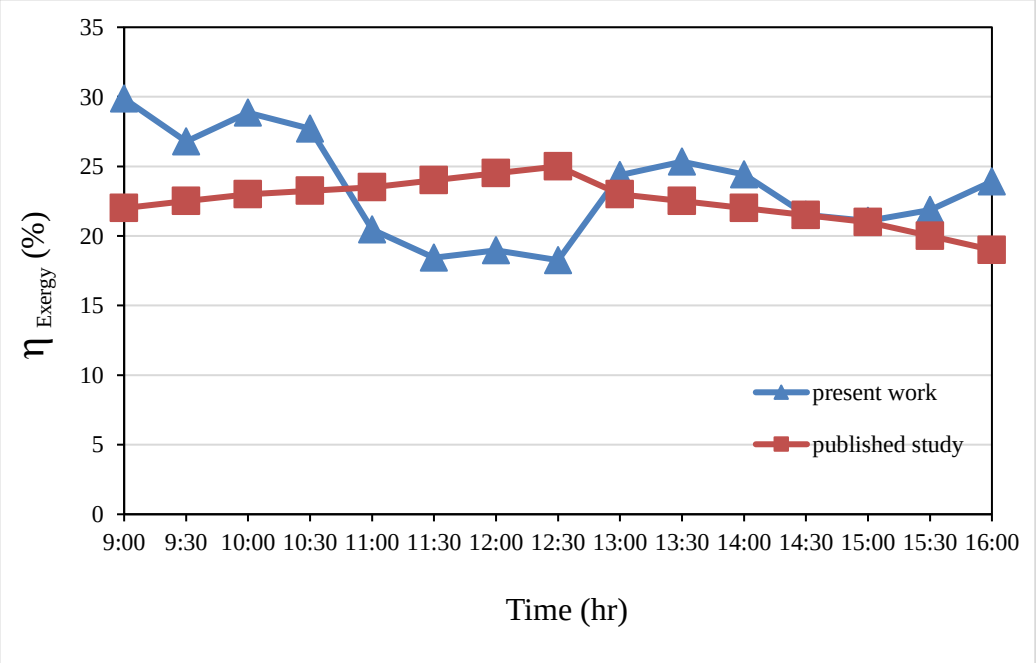

Figure 4.4.Exegetic efficiency variation with time.

4.3. SOLAR RADIATION RESULTS

4.3.1. Thermal Efficiency with Time

The performance of systems operating based on solar thermal energy is greatly affected by the levels of solar radiation falling on the absorbing plate. Therefore, it is necessary first to review the solar radiation recorded on the solar collectors, which is the important factor in calculating the thermal performance of these collectors later. Here is includes a presentation of the intensity of the solar radiation falling on the solar collectors (which was measured for the period from nine o'clock in the morning until five o'clock in the afternoon and by reading every half hour). The readings were taken in the city of Ramadi for fifteen days and for different days (clear days, partly cloudy and totally cloudy). Only the completely sunny days are shown in the figures.

The figure 4.5. A, B, C and D shows the solar radiation values falling on the solar collectors for the period of conducting the experiments for different flow rates. It is clear in the presented figures that the values of solar radiation begin to increase with the time of the day to reach its peak at noon or shortly after. After midday, the intensity of solar radiation begins to decrease until sunset. The maximum value of solar radiation has been recorded. The solar radiation during the period of operation of the experiments greatly affects the performance of solar collectors. It is clear from the figures that the highest solar radiation occurs between twelve o'clock and one o'clock and the values ranged between 750 W/m^2 on Tuesday (22/02/2022) and 970 W/m^2 on Wednesday (02/03/2022).

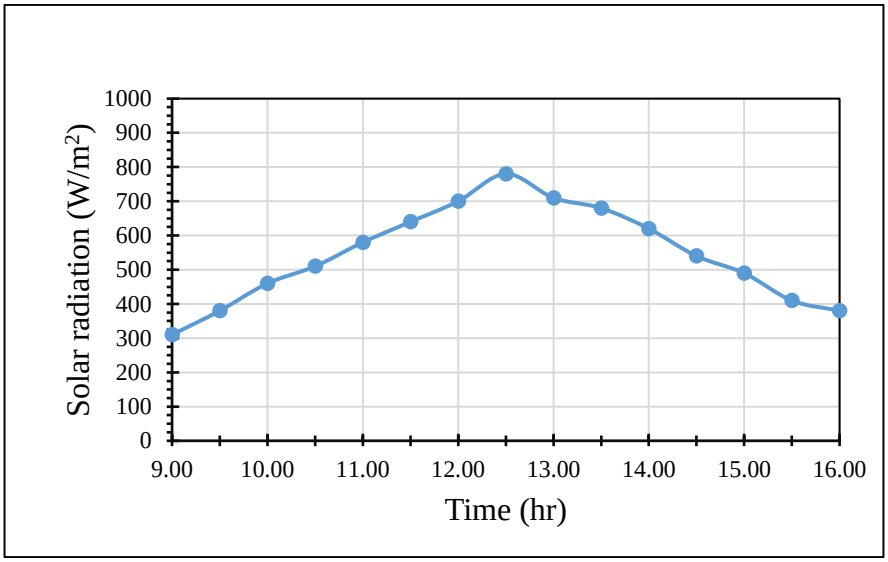
Solar radiation (W/m2)
1000
900
800
700
600
500
400
300
200
100
0
9.00
10.00
11.00
12.00
13.00
14.00
15.00
16.00
Time (hr)

(A)

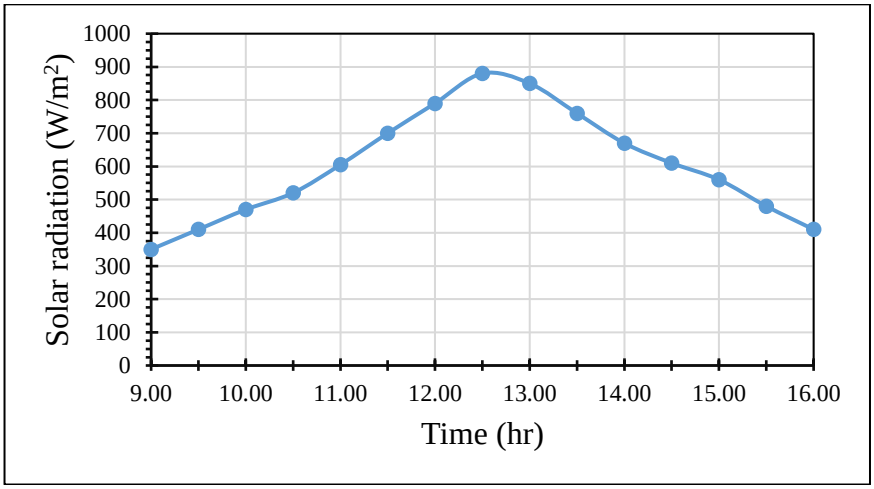
Solar radiation (W/m2)
1000
900
800
700
600
500
400
300
200
100
0
9.00
10.00
11.00
12.00
13.00
14.00
15.00
16.00
Time (hr)

(B)

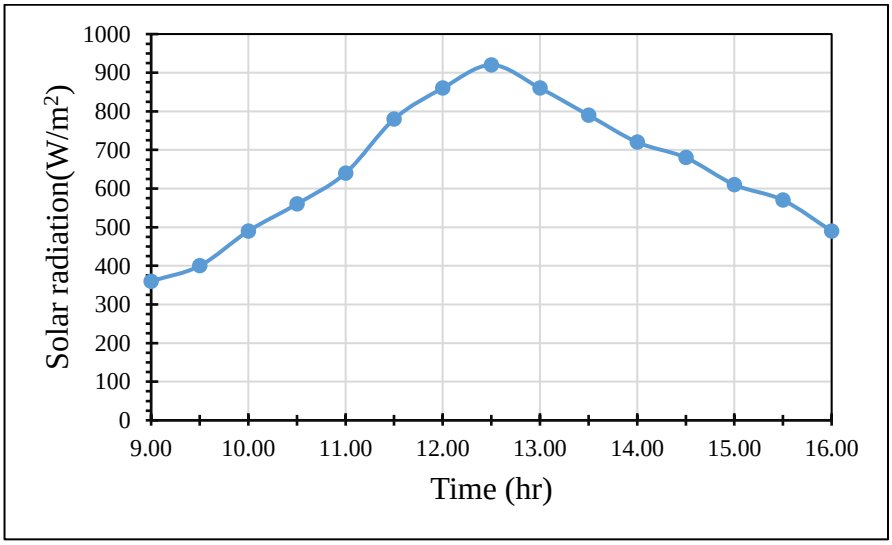
Solar radiation(W/m2)
1000
900
800
700
600
500
400
300
200
100
0
9.00
10.00
11.00
12.00
13.00
14.00
15.00
16.00
Time (hr)

(C)

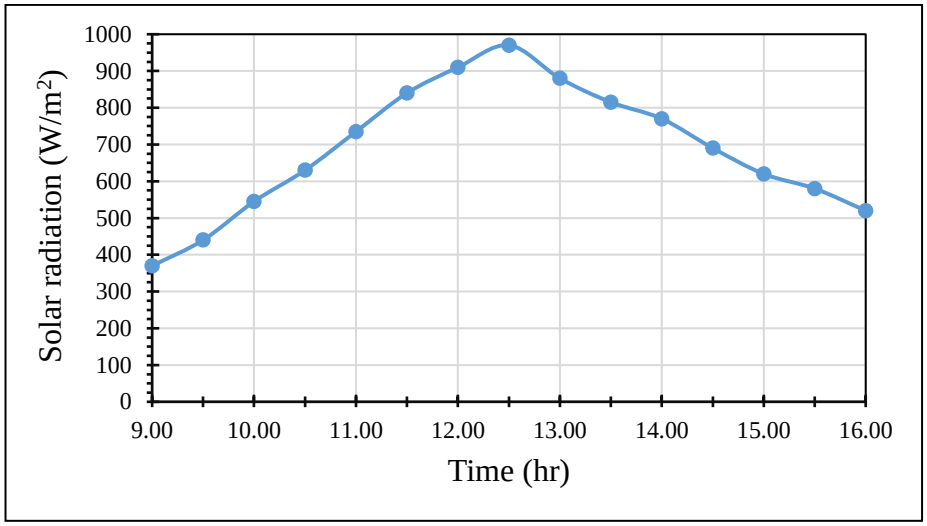

(D)

Figure 4.5. The relationship between Soler radiation and time in terms of ṁ where (A) ṁ =0.02 kg/s, (B) ṁ =0.026 kg/s, (C) ṁ =0.028 kg/s and (D) ṁ =0.03 kg/s

4.3.2. Effect of Solar Radiation on Thermal Efficiency

Because the thermal efficiency of all solar collectors is intimately tied to solar radiation, it's important to understand how they react to it. Figure 4.6 depicts the influence of various solar radiation levels on thermal efficiency throughout the experiment period. From these figures it appears that by increasing the values of solar radiation for all types of collectors led to an increase the heat gain, hence increase the thermal efficiency, and when the radiation values are low (in the morning and afternoon times close to sunset), the efficiency decreases significantly and this is due to the significant decrease in the values of heat gain at the small radiation values. Its clear that maximum Thermal Efficiency =55.99% at 12.30 p.m.

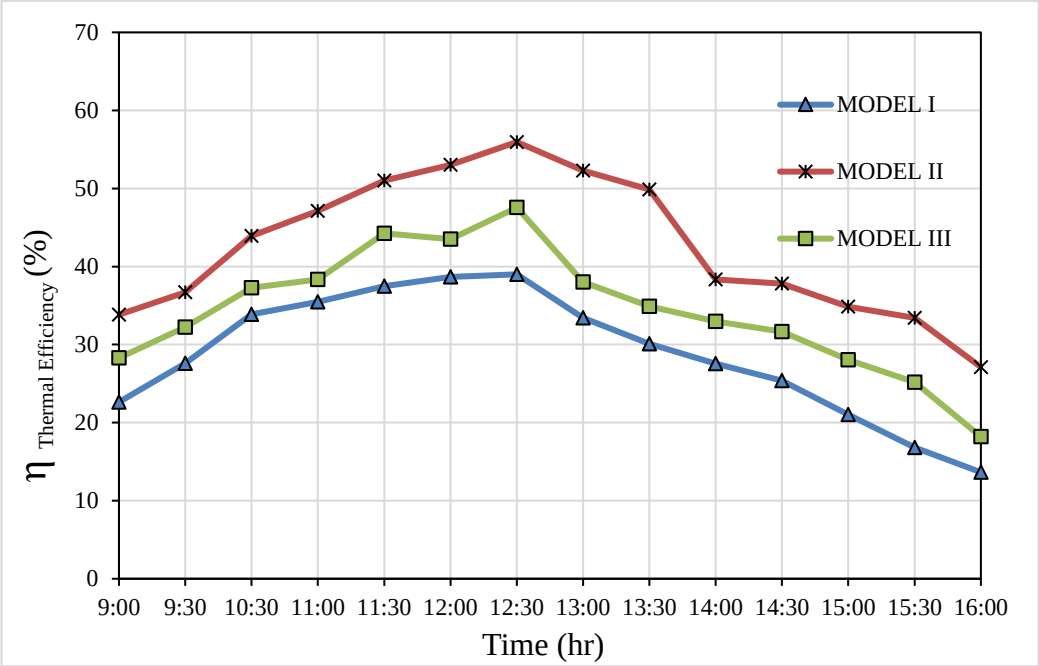

Figure 4.6. Comparison thermal efficiency with three models at $\dot{m}$ =0.020 kg/s on Tuesday (22/02/2022) .

4.4. TEMPERATURE VARIATIONS RESULTS

The temperature of the absorber plate rises as a consequence of the decrease of solar radiation on each of the three kinds of solar air collectors employed in tests, and the process of heat exchange between the air and the absorber plate starts. Conduction and convection modes of heat exchange are well-known in the heat exchange process, as is the case here. Figure 4.7, 4.8 and 4.9 show the Temperature Variations of Inlet, Outlet, Absorber plate temperature, and temperature difference for the three models used in experiments. Figure 4.7 represent the flat plate absorber (MODEL I) and it is the solar collector that will be used for the purpose of comparison with other types used in the experiments. The mass flowrate in this experiment is (0.02 kg/s) and it is the lowest value used in the experiments. From this figure, it can be seen that the behavior of the temperature of the air leaving the collector (T_{out}) is associated with the temperature of the absorber plate. It may be Note that the highest temperature value that can reach by the outside air from the collector is between twelve noon and one in the afternoon, and This is typical since the absorber plate is at its greatest temperature at this time. The biggest temperature differential between the outside and internal air is shown in the graph (T_{out}-T_{in}) which will be the basis for calculating the heat gain,

was 7°C before midday and at the end of the day it was approximately 3.5°C, and this value is relatively small.

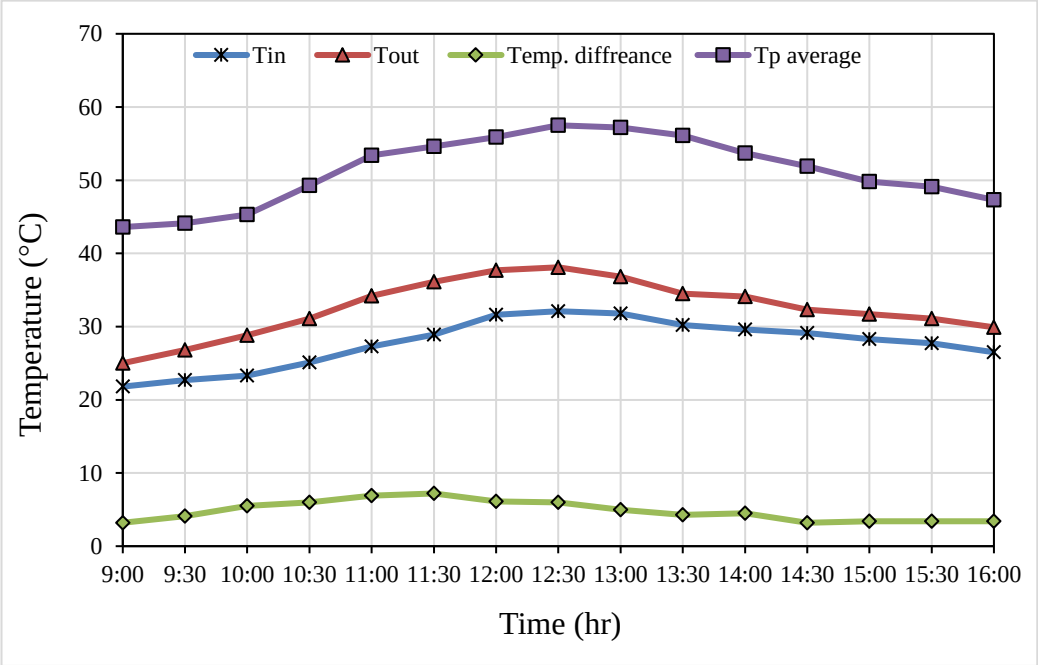

Figure 4.7. MODEL I at ṁ =0.020 kg/s on Tuesday (22/02/2022).

Figure 4.8 shows the same behavior in the distribution of temperature across daylight hour, but for the second model (MODEL II). The temperature distribution for the period of conducting the experiments shows the benefit of using metal cans in a changing arrangement, which caused an increase in air vortices, which increased the value of heat exchange resulting in a rise in the temperature of the air that exited the collector's absorbent plate. The graph illustrates that the temperature difference between the two points is the greatest the outside and inside air (T_{out}-T_{in}), which will be the basis for calculating the heat gain, was 10 °C at approximately midday and at the end of the day it was approximately 7°C.

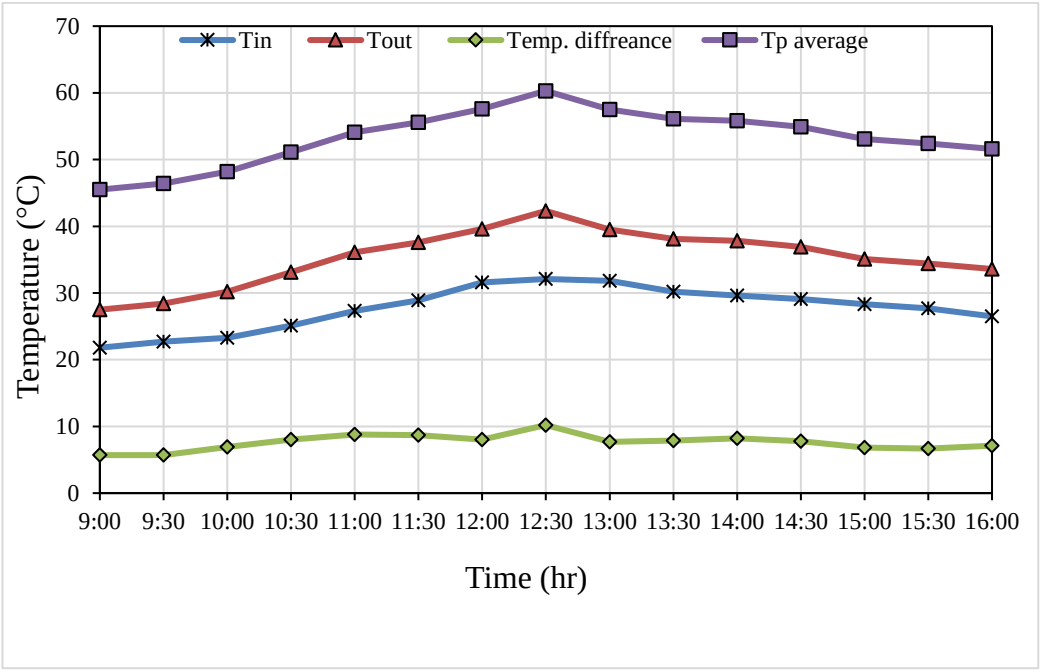

Figure 4.8. MODEL II at ṁ =0.020 kg/s on Tuesday (22/02/2022).

Figure 4.9 shows the behavior in the distribution of temperature across daylight hour for the third model (MODEL III). The improvement in the temperature value of the outside air was better in this type than in the first model, but it did not reach what the benefit reached in the second model. The figure shows that the value of (T_{out}-T_{in}) at the end of the day was approximately 5℃.

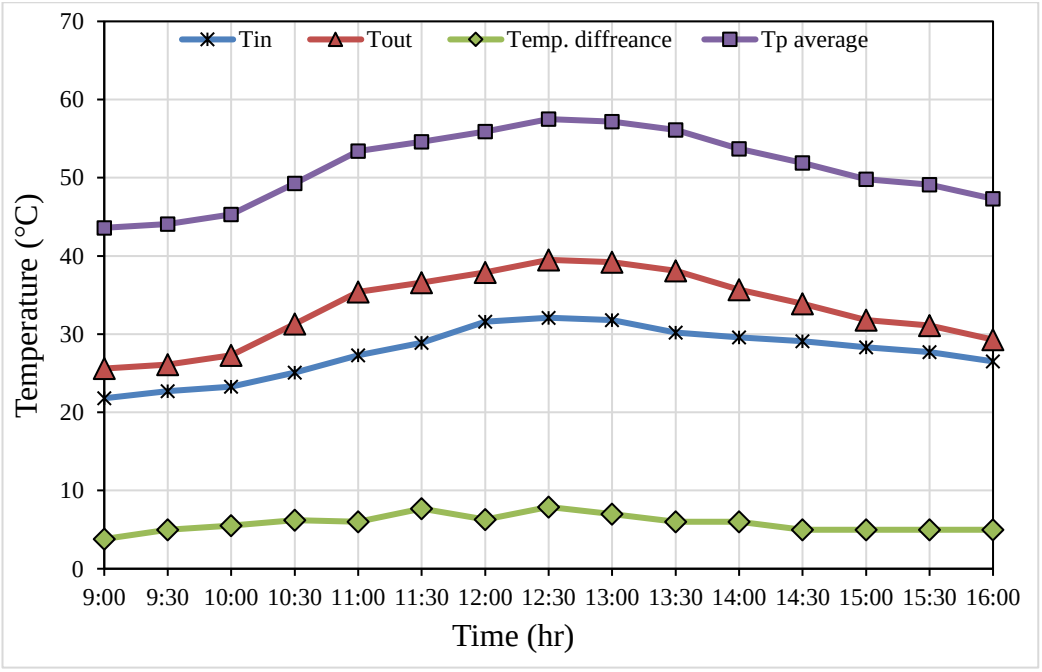

Figure 4.9. MODEL III at ṁ = 0.020 kg/s on Tuesday (22/02/2022).

Figure 4.10, 4.11 and 12 show the temperature variation in the day of (Wednesday 23/02/2022) where the mass flowrate increases to 0.026 kg/s. The figures show that the variation of inlet, outlet, difference temperatures have the same behavior as that of the absorber plate. It increases slightly at the beginning of the experiment to a maximum value at approximately midday then decreases to the end of the day. The same results for the second model occur in this figure related to the maximum temperature difference which was near 40^{o}C at midday and the value was approximately 38^{o}C at the end of the day. The temperature difference were 14^{o}C, 21^{o}C , 17^{o}C for first model, second model ,and third model respectively.

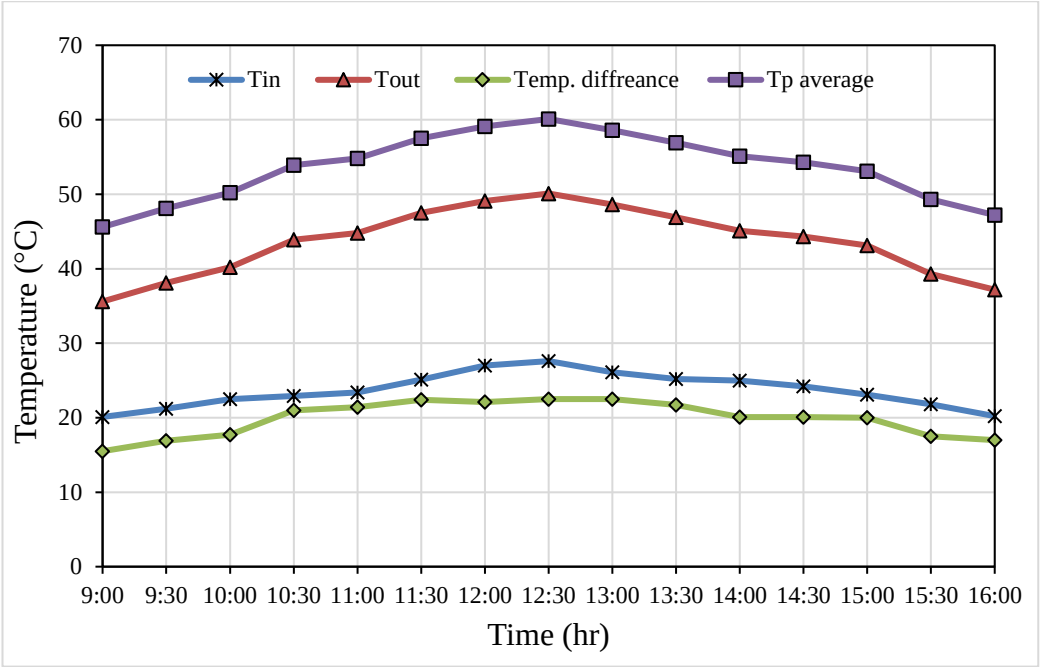

Figure 4.10. Where the $\dot{m}$ =0.026 kg/s on Wednesday (23/02/2022). (MODEL I).

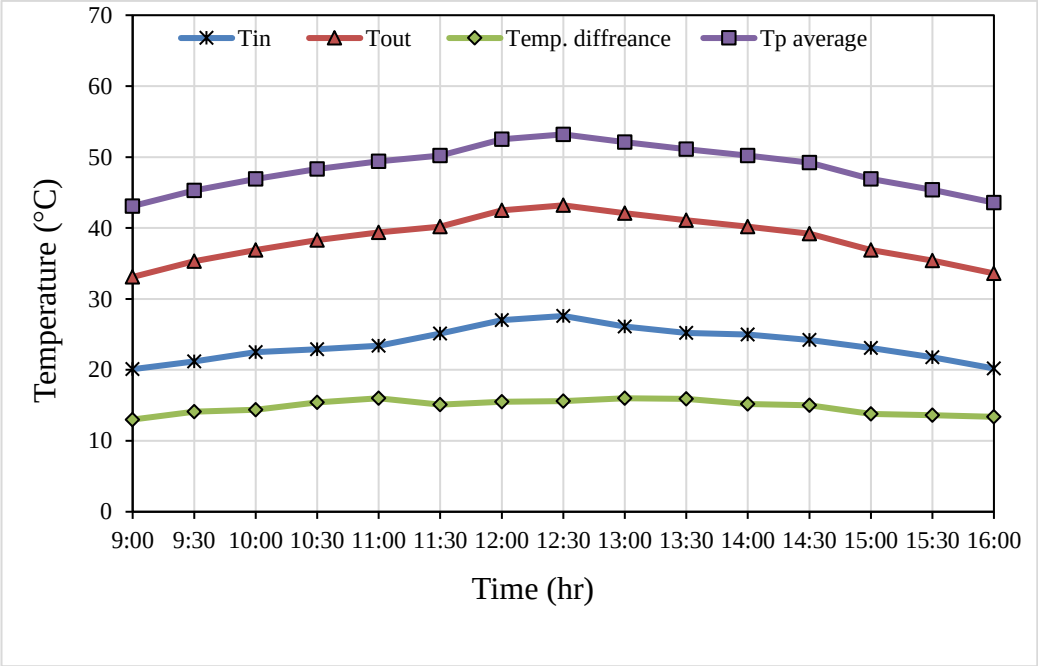

Figure 4.11.Where the ṁ =0.026 kg/s on Wednesday (23/02/2022). (M0DEL II).

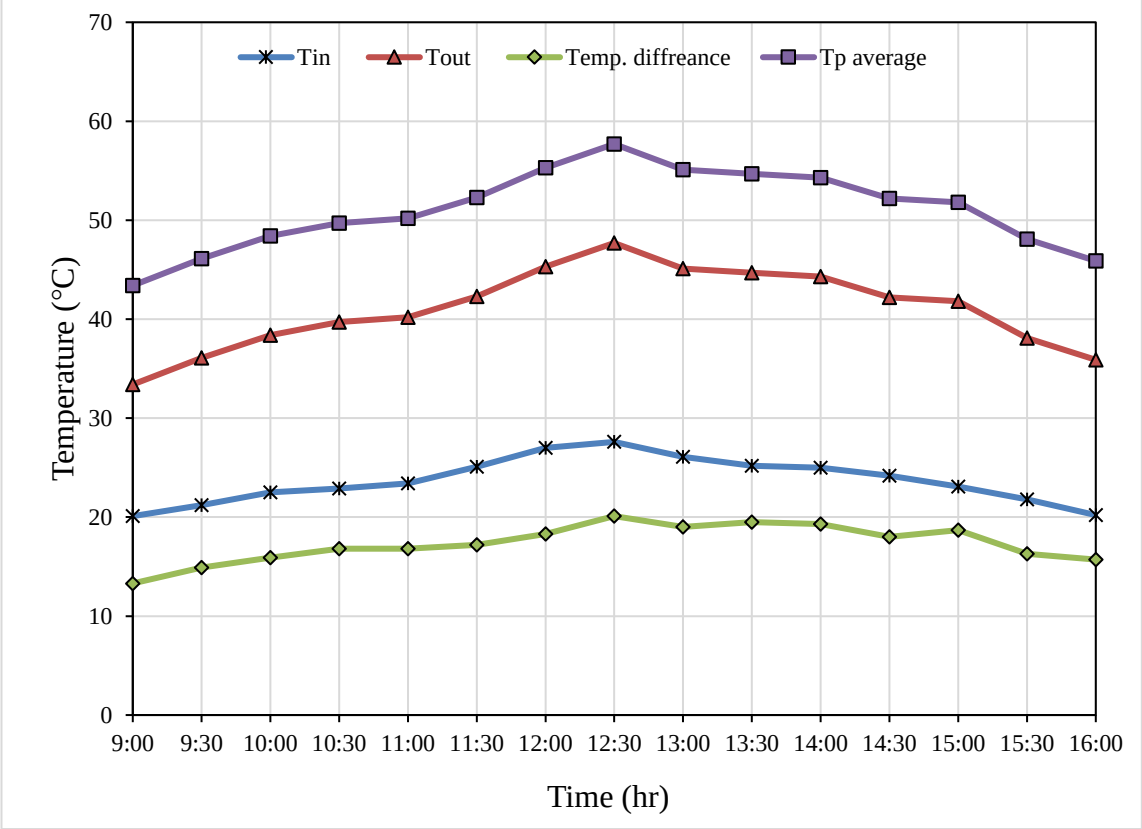

Figure 4.12.Where the mass flow rate (0.026 kg/s) in Wednesday (23/2/2022). (MODEL III).

4.5. HEAT GAIN WITH TIME

The heat gain of solar air collectors is defined as the heat value gained by the air during its passage over the absorbent plate, which leads to a higher temperature than its temperature value while entering the collector. The increase in the temperature difference between the outside air and the inside air indicates that the air has gained heat as a result of the heat exchange process (both by conduction and convection) between it and the absorber plate.

Figure 4.13, 4.14 and 4.15 indicate the variation of the heat gain of the three collectors used in experiment at mass flow rate=0.03 kg/s on (Wednesdays 02/03/2022 (from 9:00 am to 16:00 pm .The figures show that for the three types of collectors it's obvious that the heat gain increases gradually from the beginning of the experiment to the mid-day then begin to decreases gradually due to the decrease of solar radiation .It's clear that the second model gave the highest value of the heat gain .This can be explained by the shape of the metal cans placed on the absorber plate, which, in addition to increasing the area of absorption for heat radiation, created large vortices in the air, which improved the process of heat exchange between hot and cold air. The maximum heat gains = 737.2 W in 12:30 p.m in Figure 4.14 Model II.

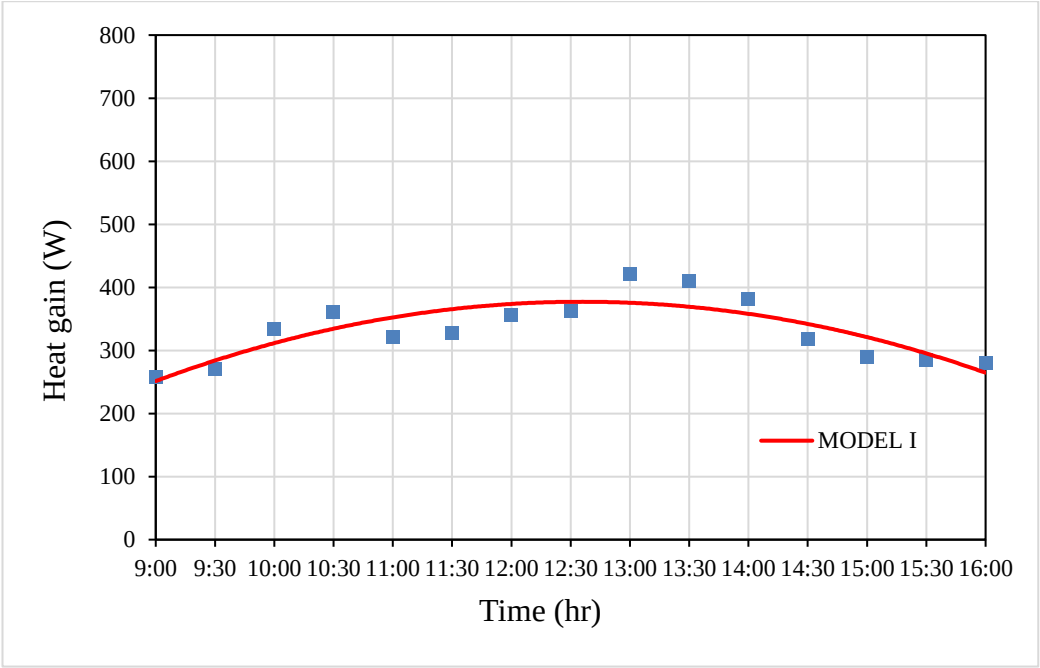

Figure 4.13. Heat Gain Verse Time for three models at $\dot{m}$ =0.03 kg/s on Wednesdays (02/03/2022) (MODEL I).

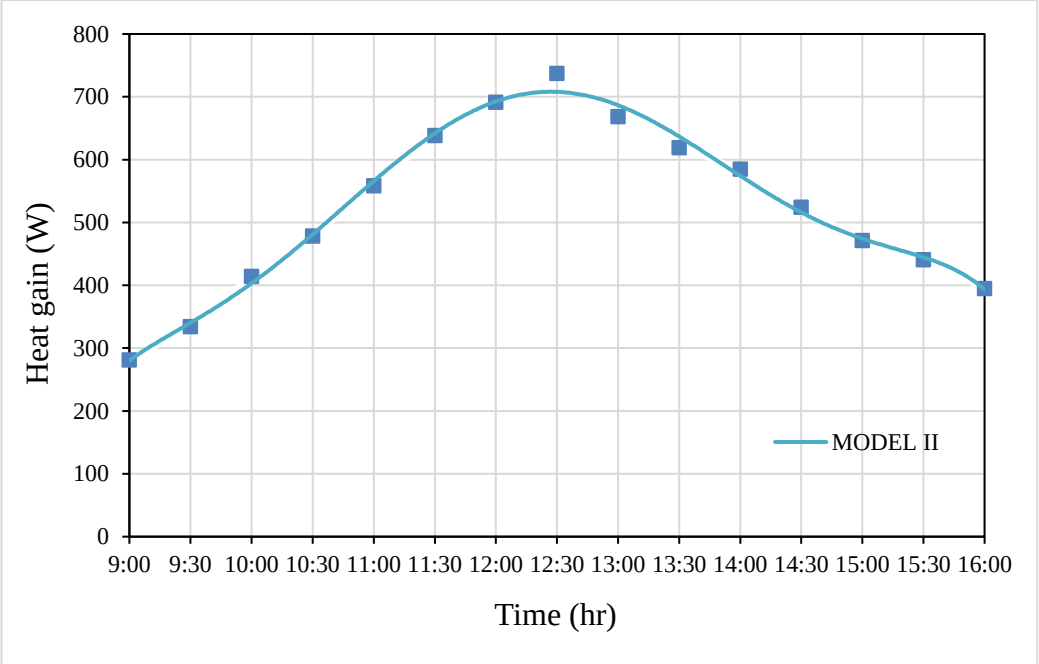

Figure 4.14. Heat Gain Verse Time for three models at ṁ =0.03 kg/s on Wednesdays (02/03/2022) (MODEL II).

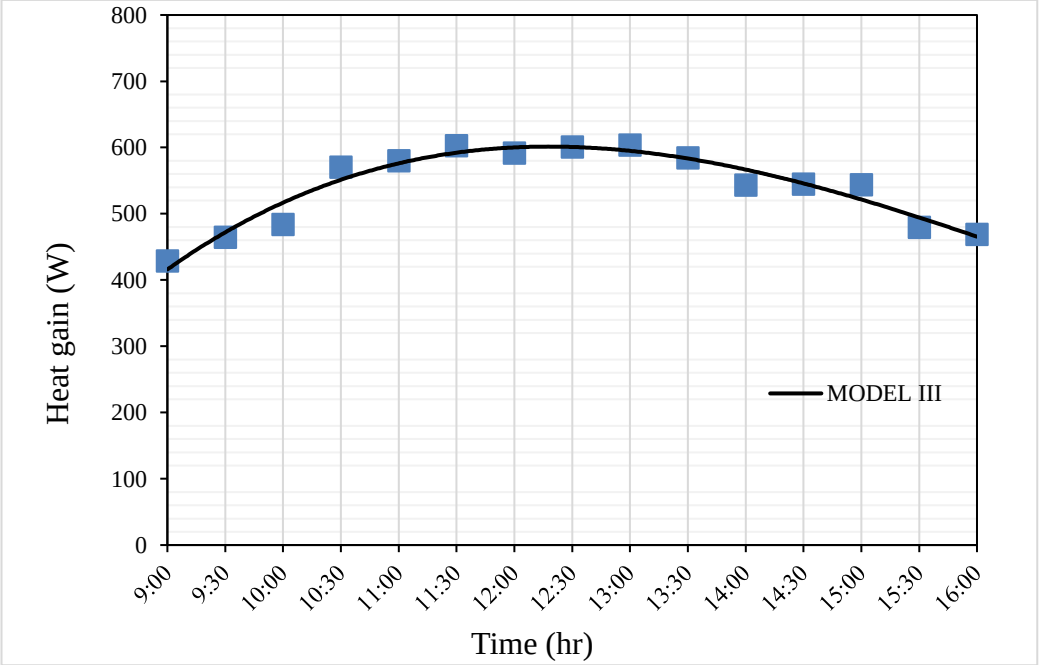

Figure 4.15. Heat Gain Verse Time for three models at ṁ = 0.03 kg/s on Wednesday (02/03/2022) (MODEL III).

4.6. THERMAL EFFICIENCY WITH TIME

Efficiency is the most important factor in evaluating solar collectors' thermal performance, which may be defined as the quantity of heat gained by air moving through the collecting a solar collector because of the temperature differential between exiting and incoming air.

Figure 4.16 shows the behavior of thermal efficiencies of the three different collector models used in experiments on a clear day on (the mass flow rate increases to 0.026 kg/s in Wednesday (23/02/2022) where from 09:00 a.m to 04:00 p.m, for every half hour through the daytime with time. From this figure, the thermal efficiency was reported to have grown to 12:30 and then started to steadily drop. The maximum thermal efficiency was 57.55%, 75.9%, 69.57% for Model I, Model II, Model III respectively at 12:30 p.m.

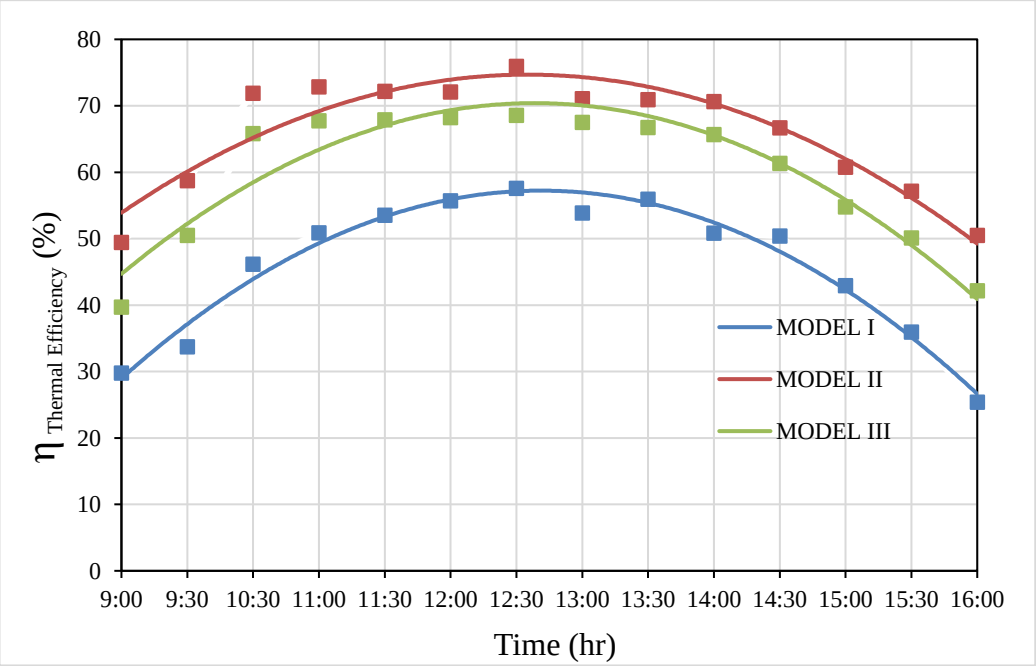

Figure 4.16. Thermal efficiency with time to three models at ṁ = 0.026 kg/s Wednesday (23/02/2022).

4.7. THERMAL EFFICIENCY AND TEMPERATURE DIFFERENCE WITH TIME

Figure 4.17 depicts the relation between the temperature difference and the thermal efficiency for the three types of collectors on a clear day on (the mass flow rate increases to 0.026 kg/s) on Wednesday (23/2/2022). Throughout the day, half-hourly presentations of the findings were made to the class. Figures showed that, due to an increase in heat gain, the thermal efficiency improved for all collector designs as the temperature differential between input and output rose. The greatest amount of time at 12:30 p.m., the temperature difference was 21°C and the thermal efficiency was 75.90%.

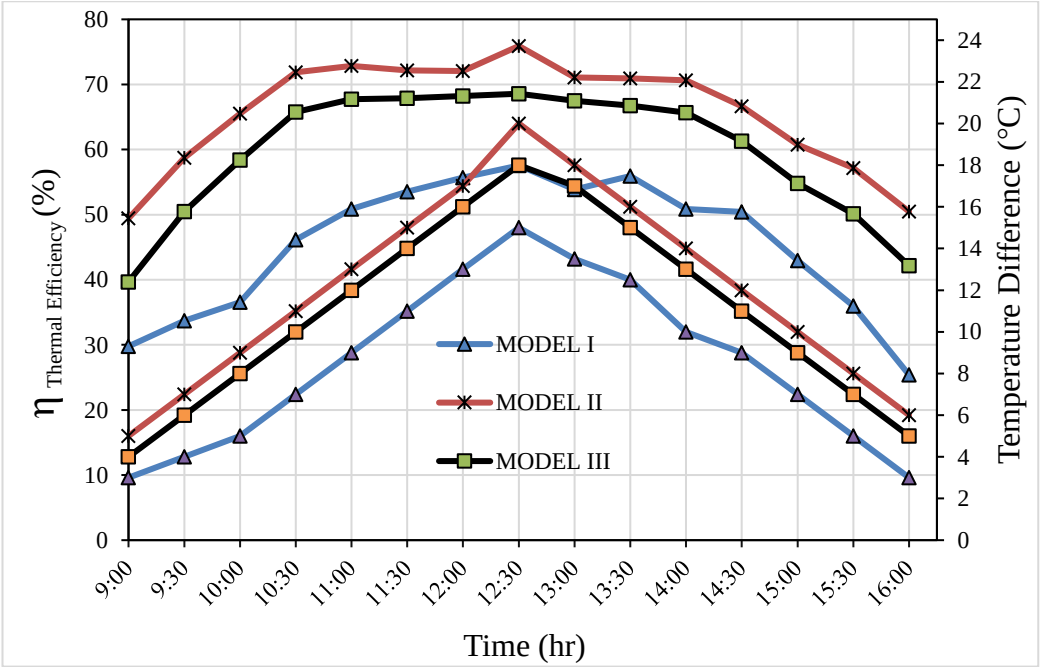

Figure 4.17. Thermal efficiency and temperature difference with time.

4.8. ENERGETIC EFFICIENCY WITH SOLAR RADIATION

The theoretical calcolations that may be done while a thermodynamic system is in exergy and thermodynamic equilibrium with its surroundings, or heat reservoir. Exergy is the highest amount of work that may be removed from a system during the exchange of matter and energy with a huge reservoir. The estimation of the efficiency of energy conversion processes based on the concept of exergy is a useful thing and present a good interpretation for the whole process. The analysis of exergy and the

exegetic efficiency gave the overcome of some defect occurs in energy analysis of any system as its present a qualitative assessment of the system.

Figure 4.18 demonstrates how solar radiation affects energy production. At ṁ =0.028 kg/s mass flow rate Tuesday, 01/03/2022, the data is shown in the image. From this graph, it can be seen that as sun radiation decreases, energy efficiency increases until noon. For Model I, Model II, and Model III, the greatest energy efficiency was 12.13%, 18 %, and 15.97 %, respectively.

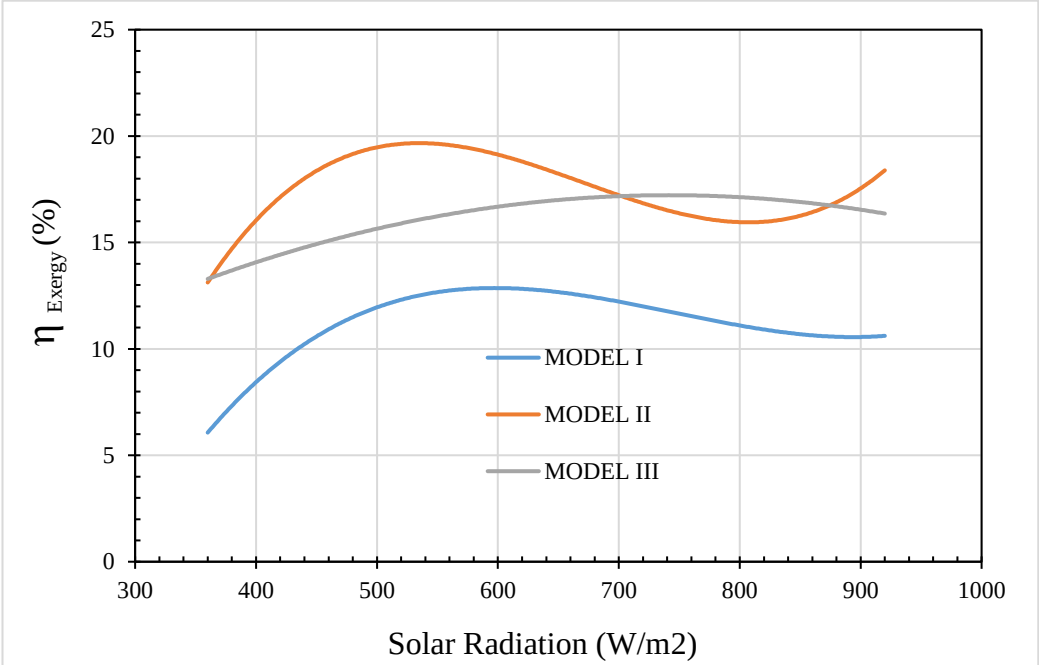

Figure 4.18. Energetic efficiency with solar radiation at Tuesday 01/03/2022 to increases at ṁ = 0.028 kg/s on 12:30 p.m. and solar radiation =920 (W/m^2).

4.9. EXEGETIC EFFICIENCY WITH TIME

In testing on Wednesday, 23/02/2022, the mass flow rate increased to 0.026 kg/s, as shown in Figure 4.19, which illustrates the exergetic efficiency for the three models that were employed. This statistic shows a rise in exergy efficiency until noon, after which it started to decline progressively. Figure 4.19 compares the exergy efficiency of three different types of exergy that were put to the test. This is what we can deduct from the graph exergy efficiency was found to be higher in Model II than the other two models. Model II has the greatest temperature difference because of the increased

heat transfer caused by the strong turbulence, resulting in the greatest temperature differential.

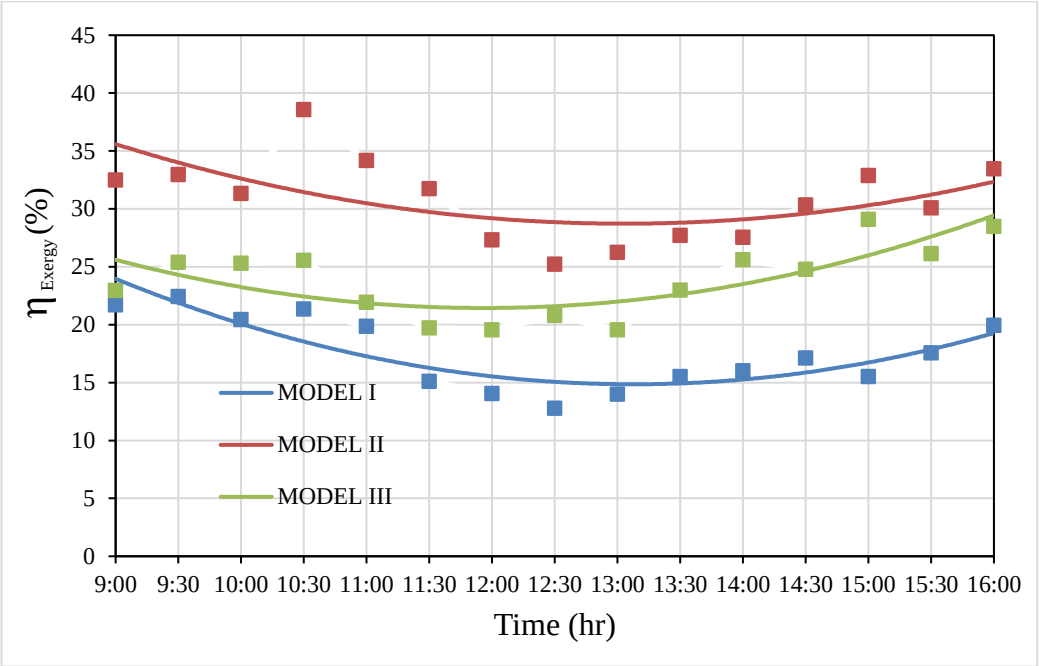

Figure 4.19. Exergetic efficiency with time to increases at $\dot{m} = 0.026$ kg/s on Wednesday (23/02/2022).

4.10. EFFECT OF MASS FLOW RATE

4.10.1. Effect of Mass Flow Rate on Thermal Efficiency

Solar collectors' efficiency is also affected by the airflow across the collection, since it represents the medium that collects heat from the absorbent plate. Four values of mass flowrate were used in experiments 0.02, 0.026, 0.028, and 0.03 kg/s. Figure 4.20 shows the thermal efficiency of several types of collectors at varying mass flowrates, with time as a function of mass flow rate. Because mass flow rate is closely connected to thermal efficiency, it was discovered that when mass flow rate increased, thermal efficiency improved. For Model III, several mass flow rates were examined, and the greatest thermal efficiency was 69.57 % at 12:30 pm for mass flow rete 0.03 kg/s.

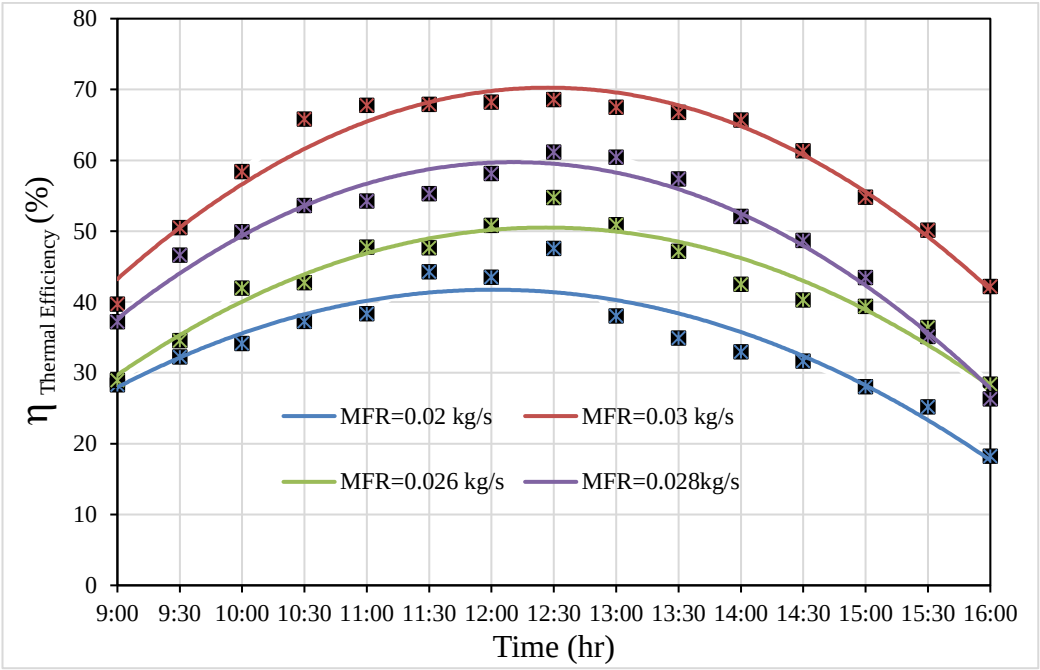

Figure 4.20. Effect of mass flow rate on thermal efficiency.

4.10.2. Effect of Mass Flow Rate on Temperatures Difference

It is shown in Figure 4.21 how the mass flow rate impacts temperature variations over time for various kinds of collectors utilized in the experiment. The temperature difference reduced as the mass flow rate increased, as seen in this graph. The lower the exit temperature, the more natural this behavior is since the shorter the time the air spends in contact with the absorber plate, the faster its velocity. Model II was used to gather readings at various mass flow rates on Tuesday, February 22nd, 2022. For mass flow rate 0.02 kg/s, the highest temperature difference was 18°C at 12:30 p.m.

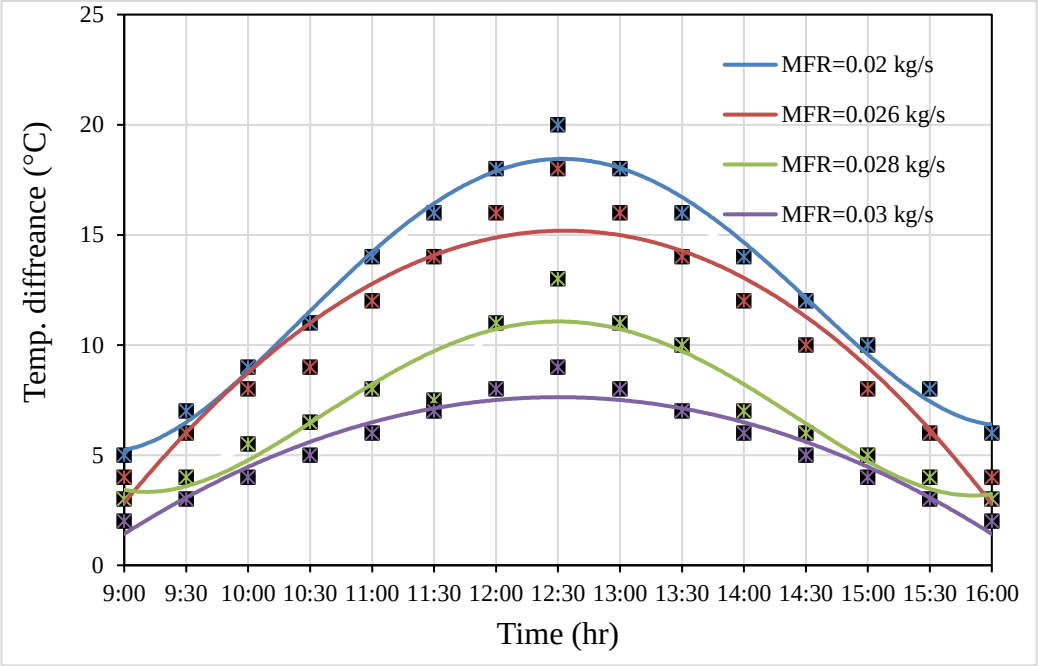

Figure 4.21. Effect of mass flow rate on temperatures difference.

4.10.3. Effect of Mass Flow Rate on Exegetic Efficiency

The influence of mass flow rate on energy efficiency over time for the three kinds of solar air heater collectors utilized in the testing is shown in Figure 4.22. Exegetic efficiency improved as the mass flow rate increased, as seen in this graph, since energetic efficiency is related to mass flow rate.

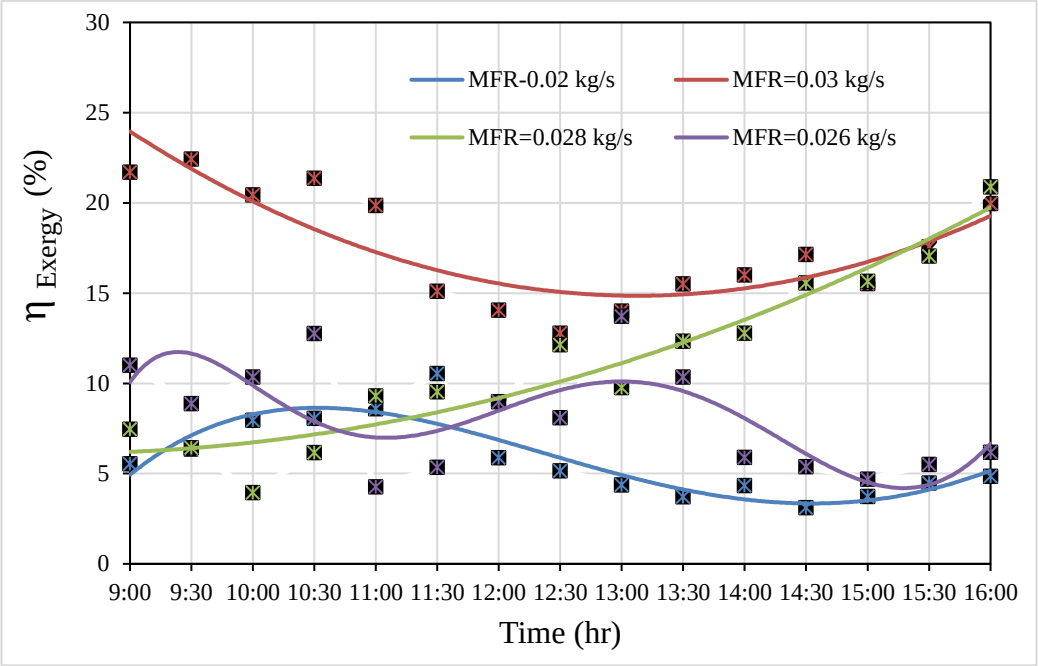

Figure 4.22. Effect of mass flow rate on exegetic efficiency.

4.10.4. Comparison of Daily Efficiency

Figure 4.23 shows a comparison of daily efficiency with a mass flow rate between the three types of collectors used in experiments. From figure Model II gave the higher daily efficiency from other types because of the higher heat transfer enhancement occurs than other two types. While Model I gave less daily efficiency because of the absorber plate has no modification. It shows the daily efficiency increase with increase mass flow rate due to increase in heat gain, which proportional from it.

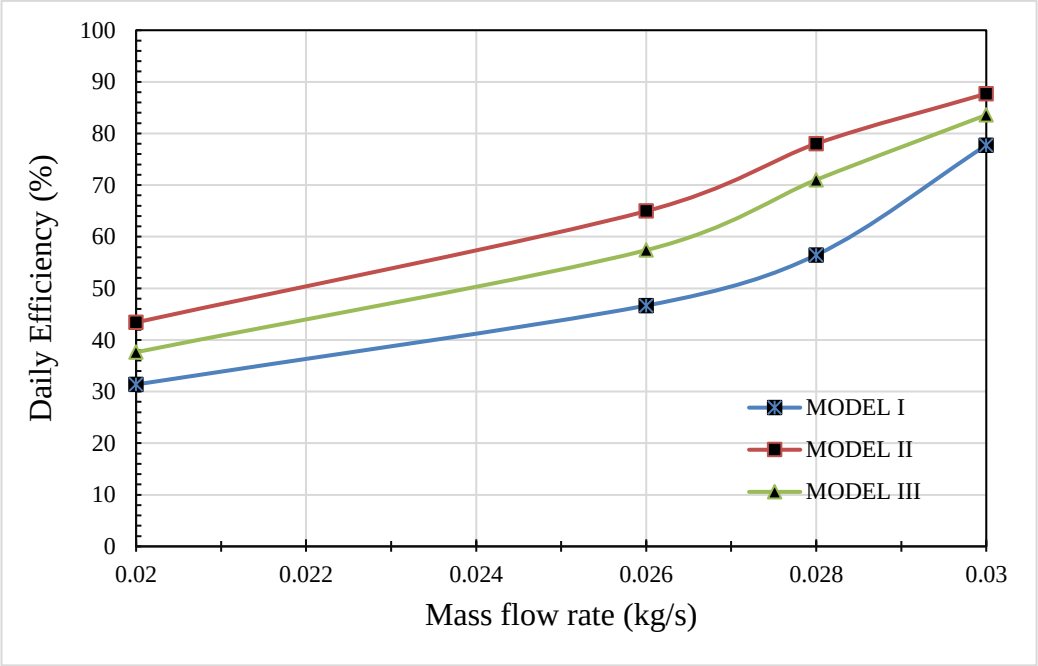

Figure 4.23. Comparison between daily efficiency.

4.11. EXEGETIC EFFICIENCY WITH TEMPERATURE DIFFERENCE PARAMETERS

One of the important parameters in clarifying the effect of solar radiation is the coefficient (The difference in temperature between leaving the collector and entering it to the incident radiation values). Figure 4.24, 4.25, 4.26 and 4.27 show the effect of ($\Delta T/I$) on the exegetic efficiency for the three types of collectors used in experiments at the various type of mass flowrate. The figures show that as ($\Delta T/I$) increases the exegetic efficiency increases for all types of collectors and the maximum exergetic efficiency occurs at mass flowrate of 0.026 kg/s and for model II. This may be interpreted as the temperature differences increases due to the increasing in solar radiation the heat gains increase leading to an increase in exergetic efficiency.

Figure 4.24 shows the effect of the exergetic efficiency and its relationship to the mass flow rate of the air used in the experiments. The exergetic efficiency improves as the mass flow rate increases, peaking at 0.026 kg/s, then declining as the flow rate rises until it hits 0.028 kg/s. This may be explained by the fact that raising the flow value causes a faster passage of air over the absorber plate, which results in a shorter heat exchange period, and hence a lower efficiency value. The chart also demonstrates that

the absorber plate model II has the highest exergetic efficiency, whereas the plain absorber plate has the lowest increase. This is expected, since the placement of the metal cans in the second model enhanced air velocity and therefore the heat exchange process, increasing the value of the heat transfer coefficient. Figure 4.24 shows similar behavior of the effect of the value of mass flowrate on the efficiency and the same interpretation may be deduced.

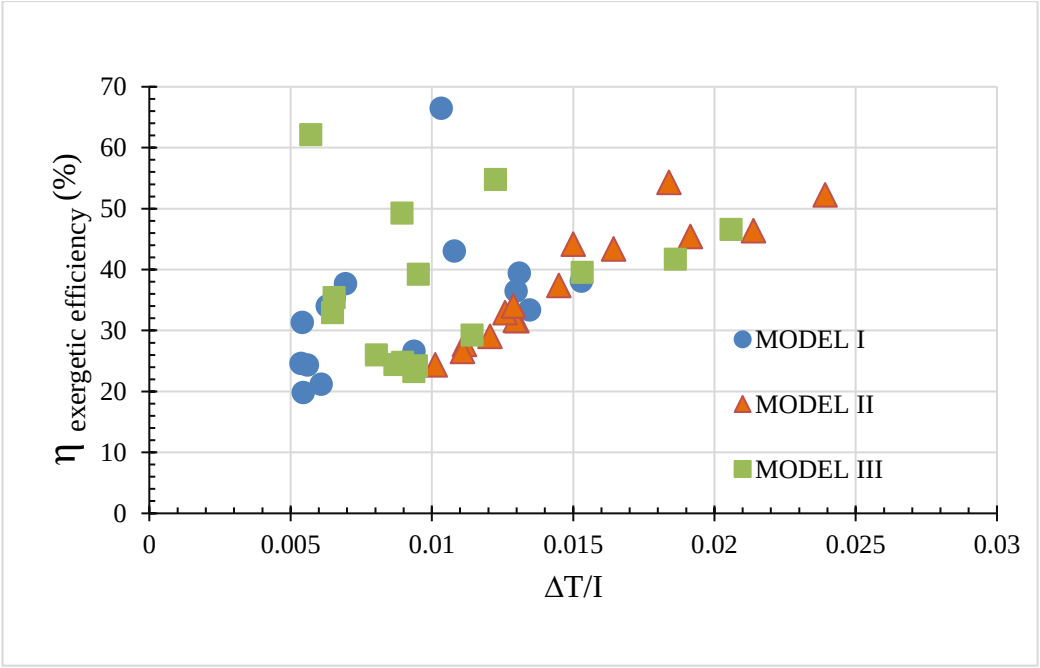

Figure 4.24. Exergetic efficiency with temperature difference parameters (°C.m^2/W) for different for three models and ṁ =0.02 kg/s.

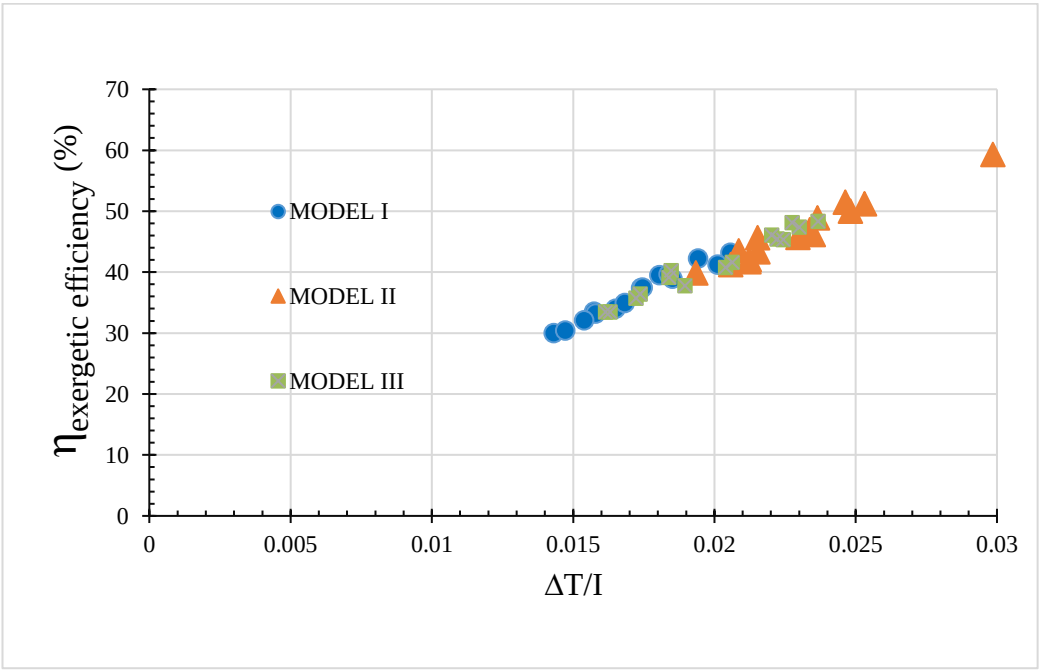

Figure 4.25. Exergetic Efficiency with temperature difference parameters (°C.m^2/W) for different for three models and ṁ =0.026 kg/s.

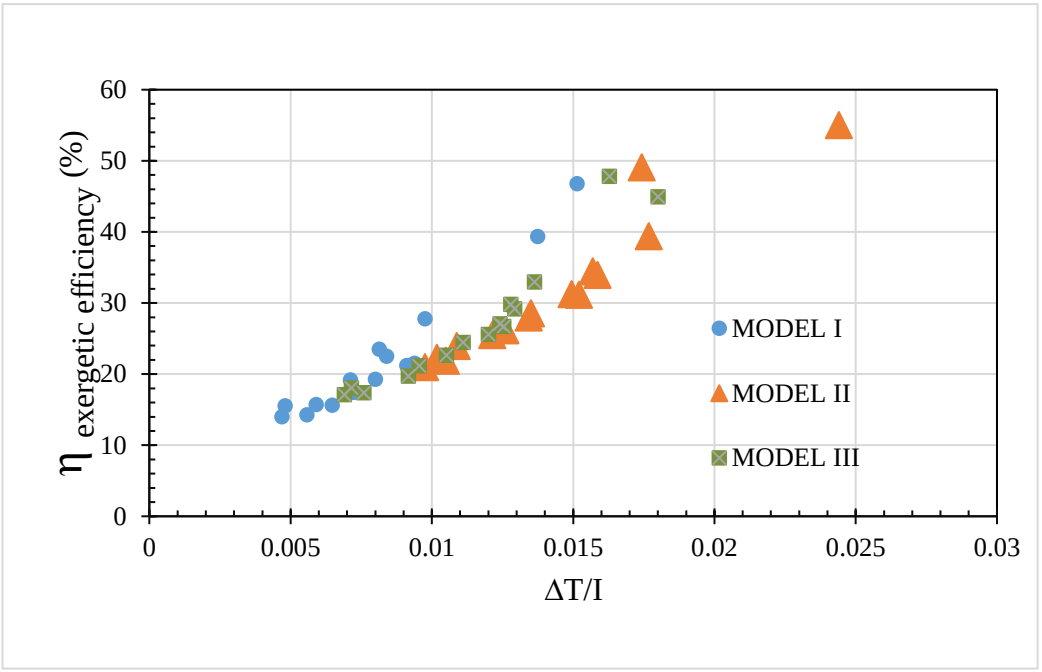

Figure 4.26. Exergetic Efficiency with temperature difference parameters (°C.m^2/W) for different for three models and ṁ =0.028 kg/s.

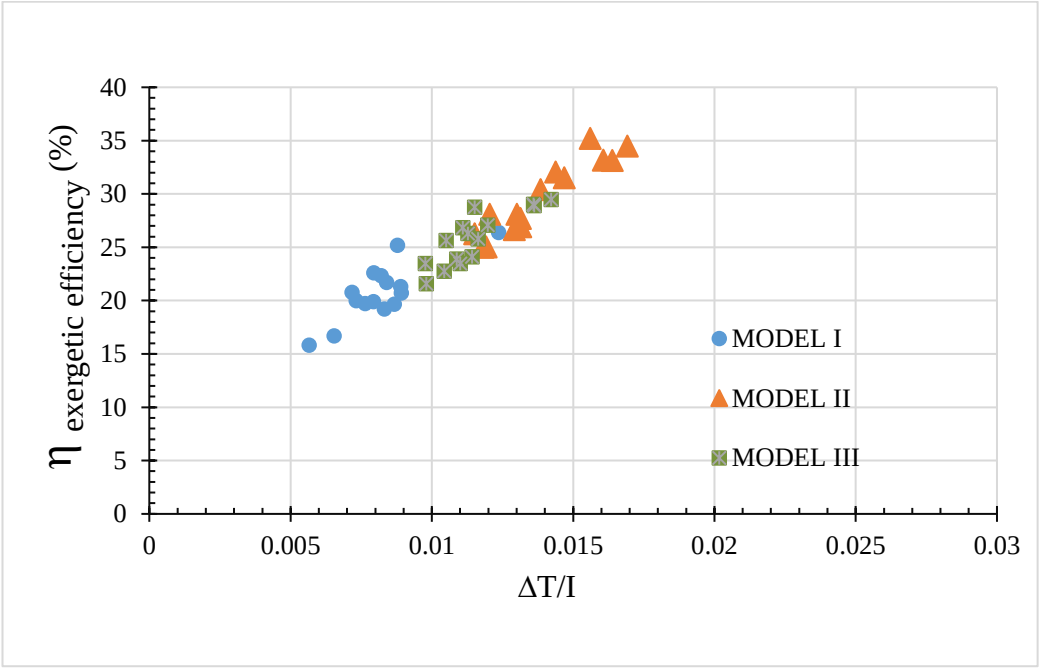

Figure 4.27. Exergetic Efficiency with temperature difference parameters (°C.m^2/W) for different for three models and ṁ =0.03 kg/s.

PART 5

CONCLUSIONS AND RECOMMENDATIONS

5.1. CONCLUSIONS

Waste metal cans were used as tabulators in an experimental setup to see how they affected double-pass collectors are more efficient than single-pass collectors. It was conducted in Anbar Governorate - Ramadi climatic conditions for the trials. An evaluation of three different designs of solar air heater absorber plates is shown and discussed. The main findings of the results as follow:

1. The use of metal cans increased the absorber plate's heat transfer area, resulting in an increase in heat transmission.
2. The increased turbulence caused by employing metal cans as extended surfaces improved the interchange of cold and hot air.
3. It is solely dependent on the values of sun irradiation and the mass air flow rate that the solar collectors' thermal efficiency is determined.
4. The higher value of the thermal efficiency obtained with Model II compared to the other two collectors.
5. The energetic efficiency obtained using Model II collector was higher than that the other two models.
6. The maximum temperature difference obtained using Model II during the experiments was 21°C.
7. The maximum temperature difference obtained at the end of experiments was 7°C using Model II solar air heater collectors.
8. The higher thermal efficiency obtained using Model II is 75.9 %.
9. The higher exergetic efficiency obtained using Model II is 38.57 %.

10. For comparing purposes of the collectors used in experiments, it was shown that Model II exhibited higher thermal efficiency, higher exergetic efficiency, and higher temperature difference at sunset.

5.2. RECOMMENDATIONS AND FUTURE WORK

When it comes to solar air heaters, there is a pressing need for improved thermal performance due to global climate change brought on by our overuse of fossil fuels. In order to better understand how these heaters, perform thermally with waste metal cans and other extended surfaces, the recommendations and future work are stated below:

1. Completing the design of the solar collector using any available software and before the system is practically fabricated, in order to clarify any weaknesses in the design and have an optimal design choice to minimize the loss of money and effort.
2. Achieving a comparative study of the theoretical models available in the open literature with the manufactured practical side.
3. Conducting a study of other different configuration of the metal cans to determine their effect on the thermal efficiency and thermal performance of the solar collector in general.
4. Depending on the solar simulator to conduct the experiments to avoid the effect of the fluctuation in solar radiation due to clouds of dust, and the effect of wind in order to study the effect of solar radiation in a stable manner.
5. Analyze the impact of various kinds of metal cans on solar air heater collector performance.
6. Conducting a complete and comprehensive economic study to compare the performance of these heaters with the traditional heaters available in the local markets.
7. Conducting a comprehensive study of the use of hot air coming out of these solar collectors in heating of a residential building, studying all factors affecting the provision of heating requirements for this building, and studying the need to add heating from another auxiliary means in the event of a decrease in the amount of hot air at night [5,47].

REFERENCES

1. Bayrak, F., Oztop, H. F., & Hepbasli, A., "Energy and exergy analyses of porous baffles inserted solar air heaters for building applications", ***Energy and Buildings,*** 5(7): 338-345 (2013).

2. Internet: Salih, S. M. Jalil, J. M. and Najim, S. I., "Experimental and numerical analysis of a double-pass solar air heater with PCM photovoltaic panels cooling view project experimental and theoretical study of novel solar air collector without and with latent heat storage view project", **https://www.researchgate.net/publication /336513218**/ (2022).

3. Krishnananth, S. S., & Murugavel, K. K., "Experimental study on double pass solar air heater with thermal energy storage", ***Journal of King Saud University-Engineering Sciences,*** 25(2): 135-140 (2013).

4. Kooli, S., Bouadila, S., Lazaar, M., & Farhat, A., "The effect of nocturnal shutter on insulated greenhouse using a solar air heater with latent storage energy", ***Solar Energy,*** 11(5): 217-228 (2015).

5. Zhu, T., Diao, Y., Zhao, Y., & Ma, C., "Performance evaluation of a novel flat-plate solar air collector with micro-heat pipe arrays (MHPA)", ***Applied Thermal Engineering,*** 11(8): 1-16 (2017).

6. Abdullah, A. S., Amro, M. I., Younes, M. M., Omara, Z. M., Kabeel, A. E., & Essa, F. A., "Experimental investigation of single pass solar air heater with reflectors and turbulators", ***Alexandria Engineering Journal,*** 59(2): 579-587 (2020).

7. Kabeel, A. E., Hamed, M. H., Omara, Z. M., & Kandeal, A. W., "Influence of fin height on the performance of a glazed and bladed entrance single-pass solar air heater", ***Solar Energy,*** 16(2): 410-419 (2018).

8. Mahmood, A. J., & Aldabbagha, L. B. Y., "Single pass solar air heater with transverse fins and without absorber plate", ***HEFAT,*** 2(10):1-2 (2012).

9. Şevik, S., & Abuşka, M., "Enhancing the thermal performance of a solar air heater by using single-pass semi-flexible foil ducts", ***Applied Thermal Engineering,*** 17(9): 115-746 (2020).

10. Adil, M., Ibrahim, O., Hussein, Z., & Waleed, K., "Experimental investigation of SAHs solar dryers with zigzag aluminum cans", ***Int J Energy Power Eng,*** *4*(5): 240-247 (2015).

11. Ozgen, F., Esen, M., & Esen, H., "Experimental investigation of thermal performance of a double-flow solar air heater having aluminum cans", ***Renewable Energy,*** 34(11): 2391-2398 (2009).

12. Mohamad, A. A., "High efficiency solar air heater", ***Solar Energy,*** 60(2): 71-76 (1997).

13. Internet: Hassan, J. M., Qussai, D., Abdul-Ghafour, J. and Mohammed, A. A. "Advances in natural and applied sciences experimental performance of a double pass solar air heater with thermal storage", **http://www.aensiweb.com/ANAShttp://creativecommons.org/licenses/by/4.0/** (2022).

14. Esen, H., "Experimental energy and exergy analysis of a double-flow solar air heater having different obstacles on absorber plates", ***Building and Environment,*** *43*(6): 1046-1054 (2008).

15. Patel, J. K. and Patel, J. D., "Experimental Investigation of Double Pass Solar Air Heater Using Multiple Aluminium Obstructions-IJAERD," ***International Journal of Advance Engineering and Research Development,*** 3(10): 4–14 (2016).

16. Chabane, F., Moummi, N., & Benramache, S., "Experimental study of heat transfer and thermal performance with longitudinal fins of solar air heater", ***Journal of Advanced Research,*** 5(2): 183-192 (2014).

17. Oztop, H. F., Bayrak, F., & Hepbasli, A., "Energetic and exergetic aspects of solar air heating (solar collector) systems", ***Renewable and Sustainable Energy Reviews,*** 2(1): 59-83 (2013).

18. Velmurugan, P., & Kalaivanan, R., "Energy and exergy analysis in double-pass solar air heater", ***Sādhanā,*** 41(3): 369-376 (2016).

19. Mahmood, A. J., & Aldabbagh, L. B. Y., "Double Pass Solar Air Heater with Transvers Fins and without Absorber Plate", ***Int. J. Mech. Aerospace, Ind. Mechatron. Manuf. Eng,*** 7(2): 1293-1298 (2013).

20. Ho, C. D., Chang, H., Lin, C. S., Chao, C. C., & Tien, Y. E., "Device performance improvement of double-pass wire mesh packed solar air heaters under recycling operation conditions", ***Energies,*** *9*(2): 6-8 (2016).

21. Wu, W., Dai, S., Liu, Z., Dou, Y., Hua, J., Li, M. & Wang, X., "Experimental study on the performance of a novel solar water heating system with and without PCM", ***Solar Energy,*** 17(1): 604-612 (2018).

22. Budea, S., "Solar air collectors for space heating and ventilation applications—performance and case studies under Romanian climatic conditions", ***Energies,*** *7*(6): 3781-3792 (2014).

23. Yeh, H. M., & Ho, C. D., "Collector efficiency in downward-type double-pass solar air heaters with attached fins and operated by external recycle", ***Energies,*** *5*(8): 2692-2707 (2012).

24. Kurtbas, I., & Turgut, E., "Experimental investigation of solar air heater with free and fixed fins: efficiency and exergy loss", ***International Journal of Science & Technology,*** 1(1): 75-82 (2006).

25. Saha, S. N., & Sharma, S. P., "Performance evaluation of corrugated absorber double flow solar air heater based on energy, effective and exergy efficiencies", ***International Journal of Mechanical & Mechatronics Engineering,*** 17(1): 63-76 (2017).

26. Bayrak, F. and Oztop, H. F., "Experimental analysis of thermal performance of solar air collectors with aluminum foam obstacles", ***J. of Thermal Science and Technology,*** 3(5): 11–20 (2015).

27. Kumar, R., & Kumar, A., "A parametric study of the 2D model of solar air heater with elliptical rib roughness using CFD", ***Journal of Mechanical Science and Technology,*** *31*(2): 959-964 (2017).

28. Dogra, S., Jilte, R. D., & Sharma, A., "Study of Performance Enhancement of Single and Double Pass Solar Air Heater with Change in Surface Roughness", ***In Journal of Physics: Conference Series,*** 15(31):12-91 (2020).

29. Gupta, B., Waiker, J. K., Manikpuri, G. P., & Bhalavi, B. S., "Experimental analysis of single and double pass smooth plate solar air collector with and without porous media", ***American Journal of Engineering Research,*** 2(12): 144-149 (2013).

30. Ramani, B. M., Gupta, A., & Kumar, R., "Performance of a double pass solar air collector", ***Solar Energy,*** 84(11): 1929-1937 (2010).

31. Vyas, S., & Punjabi, S., "Experimental study of thermal performance enhancement of a flat plate solar air heater using optical measurement technique", ***International Journal of Recent Advances in Mechanical Engineering***, 4(3): 81-97 (2015).

32. Al-Damook, M., Obaid, Z. A. H., Al Qubeissi, M., Dixon-Hardy, D., Cottom, J., & Heggs, P. J., "CFD modeling and performance evaluation of multipass solar air heaters", ***Numerical Heat Transfer, Part A: Applications,*** 76(6): 438-464 (2019).

33. Kabeel, A. E., Hamed, M. H., Omara, Z. M., & Kandeal, A. W., "Influence of fin height on the performance of a glazed and bladed entrance single-pass solar air heater", ***Solar Energy,*** 16(2): 410-419 (2018).

34. Skullong, S., Kwankaomeng, S., Thianpong, C., & Promvonge, P., "Thermal performance of turbulent flow in a solar air heater channel with rib-groove turbulators", ***International Communications in Heat and Mass Transfer,*** 5(10): 34-43 (2014).

35. Rohsenow, W. M., Hartnett, J. P., & Cho, Y. I., "Handbook of heat transfer", ***McGraw-Hill,*** New York, 12-22 (1998).

36. Mackay, K. K., Najjar, F. M., Ali, S. J., Eggert, J. H., Haxhimali, T., Morgan, B. E., & Saunders, A. M., "Hydrodynamic computations of high-power laser drives generating metal ejecta jets from surface grooves", ***Journal of Applied Physics,*** 128(21): 215-904 (2020).

37. Internet: Kapardar, A. K. and Sharma, R. P., "Experimental investigation of solar air heater using porous medium international journal of mechanical engineering and technology", **www.jifactor.com/**(2022)**.**

38. Duffie, J. A., & Beckman, W. A., "Solar engineering of thermal processes", ***Wiley,*** New York, 16-91 (1980).

39. Karsli, S., "Performance analysis of new-design solar air collectors for drying applications", ***Renewable Energy,*** 32(10): 1645-1660 (2007).

40. Internet: Salih, S. M., Jalil, J. M. and Najim, S. I., "Experimental and numerical analysis of a double-pass solar air heater with PCM photovoltaic panels cooling view project experimental and theoretical study of novel solar air collector without and with latent heat storage view project", **https://www.researchgate.net/ publication /336513218/** (2022).

41. Lin, W., Gao, W., & Liu, T., "A parametric study on the thermal performance of cross-corrugated solar air collectors", ***Applied Thermal Engineering,*** 26(10): 1043-1053 (2006).

42. Gao, W., Lin, W., Liu, T., & Xia, C., "Analytical and experimental studies on the thermal performance of cross-corrugated and flat-plate solar air heaters", ***Applied Energy,*** *84*(4): 425-441 (2007).

43. Akpinar, E. K., & Koçyiğit, F., "Energy and exergy analysis of a new flat-plate solar air heater having different obstacles on absorber plates", ***Applied Energy,*** 87(11): 3438-3450 (2010).

44. Alabdeen Z. Obaid, H., Al-Damook, A. and Khalil, W. H., "The thermal and economic characteristics of solar air collectors with different delta turbulators arrangement," ***Heat Transfer - Asian Research,*** 48(6): 2082–2104 (2019).

45. Khalil, W. H., Obaid, Z. A. H., & Dawood, H. K., "Exergy analysis of single-flow solar air collectors with different configurations of absorber plates", ***Heat Transfer—Asian Research,*** 48(8): 3600-3616 (2019).

46. Farhan, A. A., Obaid, Z. A. H., & Hussien, S. Q., "Analysis of exergetic performance for a solar air heater with metal foam fins", ***Heat Transfer,*** 49(5): 3190-3204 (2020).

47. Salih, S. M., Jalil, J. M., & Najim, S. E., “Experimental and numerical analysis of double-pass solar air heater utilizing multiple capsules PCM”, ***Renewable Energy,*** 143, 1053-1066 (2019).

RESUME

Haitham Ghassan YASEEN was born in Anbar and he graduated primary, elementary, and high school in this city, after that, he started the College of Engineering, Department of Mechanical Engineering in University of Anbar in 2000. Then in 2020, he started at Karabuk University Mechanical Engineering to complete his M. Sc. education.